ORNL/TM-2017/57

The D-D Neutron Generator as an Alternative to Am(Li) Isotopic Neutron Source in the Active Well Coincidence Counter

Robert D. McElroy Jr.
Steve L. Cleveland

January 2017

OAK RIDGE NATIONAL LABORATORY
MANAGED BY UT-BATTELLE FOR THE US DEPARTMENT OF ENERGY

ORNL/TM-2017/57

Nuclear Security and Isotope Technology Division

THE D-D NEUTRON GENERATOR AS AN ALTERNATIVE TO AM(LI) ISOTOPIC NEUTRON SOURCE IN THE ACTIVE WELL COINCIDENCE COUNTER

Robert D. McElroy, Jr.
Steve Cleveland

Date Published: January 2017

Prepared by
OAK RIDGE NATIONAL LABORATORY
Oak Ridge, TN 37831-6283
managed by
UT-BATTELLE, LLC
for the
US DEPARTMENT OF ENERGY
under contract DE-AC05-00OR22725

CONTENTS

LIST OF FIGURES

LIST OF TABLES

ABBREVIATED TERMS

AWCC	Active Well Coincidence Counter
COTS	commercial off-the-shelf
DD/AWCC	deuterium-deuterium neutron generator/Active Well Coincidence Counter
DU	depleted uranium
HDPE	high density polyethylene
JSR	Jomar Shift Register
LEU	low enriched uranium
HEU	highly enriched uranium
LV-AWCC	Large Volume Active Well Coincidence Counter
LVPS	low voltage power supply
MCNP	Monte Carlo N-Particle software package
MCS	Multi-Channel Scaler
NBL	New Brunswick Laboratory
NBS	National Bureau of Standards
NDA	nondestructive assay
ORNL	Oak Ridge National Laboratory
UNCL	Uranium Neutron Coincidence Collar

ACKNOWLEDGMENTS

This material is based upon work supported by the NA-241's Next Generation Safeguards Initiative within the Office of Nonproliferation and Arms Control, National Nuclear Security Administration, US Department of Energy for providing funding for this work.

EXECUTIVE SUMMARY

The ^{235}U mass assay of bulk uranium items, such as oxide canisters, fuel pellets, and fuel assemblies, is not achievable by traditional gamma-ray assay techniques due to the limited penetration of the item by the characteristic ^{235}U gamma rays. Instead, fast neutron interrogation methods such as active neutron coincidence counting must be used. For international safeguards applications, the most commonly used active neutron systems, the Active Well Coincidence Counter (AWCC), Uranium Neutron Collar (UNCL) and ^{252}Cf Shuffler, rely on fast neutron interrogation using an isotopic neutron source [i.e., ^{252}Cf or Am(Li)] to achieve better measurement accuracies than are possible using gamma-ray techniques for high-mass, high-density items. However, the Am(Li) sources required for the AWCC and UNCL systems are no longer manufactured, and newly produced systems rely on limited supplies of sources salvaged from disused instruments. The ^{252}Cf shuffler systems rely on the use of high-output ^{252}Cf sources, which while still available have become extremely costly for use in routine operations and require replacement every five to seven years. Lack of a suitable alternative neutron interrogation source would leave a potentially significant gap in the safeguarding of uranium processing facilities. In this work, we made use of Oak Ridge National Laboratory's (ORNL's) Large Volume Active Well Coincidence Counter (LV-AWCC) and a commercially available deuterium-deuterium (D-D) neutron generator to examine the potential of the D-D neutron generator as an alternative to the isotopic sources. We present the performance of the LV-AWCC with D-D generator for the assay of ^{235}U based on the results of Monte Carlo N-Particle (MCNP) simulations and measurements of depleted uranium (DU), low enriched uranium (LEU), and highly enriched uranium (HEU) items.

Project Status

Project status as of the time of publication:

- The LV-AWCC was modified to accept the Thermo-Fisher MP320 Pulsed Neutron Generator.
- MCNP models of the as-built DD/AWCC system were created.
- Simulations of various uranium masses, enrichments, and densities were performed to provide a broad understanding of the system response and performance capabilities.
- Measurements of a DU, LEU, HEU, ^{233}U, and Pu items were performed to validate the MCNP simulations and provide measured performance values for the DD/AWCC.
- The performance of the DD/AWCC has been evaluated for three different operating modes.
  - Active coincidence counting
  - Delayed neutron counting (using the ^{252}Cf shuffler timing sequence)
  - High repetition rate delayed neutron counting
- The high repetition rate delayed neutron counting mode was found to exceed the performance achieved by the Am(Li)-based AWCC assay for the same measurement times.
- Performances of the DD/AWCC in coincidence counting mode and traditional delayed neutron counting modes were found to be limited by the physical dimensions of the MP320 generator tube.

Operation as an Active Well Coincidence Counter (AWCC)

- Measurement accuracy was found to be similar to that of the traditional AWCC. In this mode, the neutron generator is operated in steady state mode with a neutron yield of 2E5 n/s.
- Measurement precision of the DD/AWCC operated as a traditional active coincidence counter was a factor of 2 greater (poorer) than that obtained from the LV-AWCC using Am(Li) sources. This loss of precision was determined to be the result of the large physical size of the MP320 neutron generator tube. It was not possible to shield the neutron detectors sufficiently from the source.

    - A more compact generator tube would improve this performance.

- The DD generator average neutron energy is sufficient to induce fission in ^{238}U. This sensitivity was found to be relatively small (3.9% of the response per gram compared to ^{235}U). For HEU, this sensitivity is small compared to the measurement precision observed. For LEU and DU items, it will be necessary to correct for the presence of ^{238}U.
- Passive pre-counting of the sample (i.e., generator off) allows correction for spontaneous fission events in the sample.
    - This is an important advantage over the Am(Li)-based system. For example, the spontaneous fission rate from a 18 kg DU cylinder provides the same coincidence rate as 200 g ^{235}U during active interrogation with the Am(Li) sources.

Delayed Neutron Counting: Low Repetition Rate (Shuffler) Mode

- In low repetition rate mode, the neutron generator was operated at an effective pulse rate of 0.025 Hz (irradiation times of 20 s per cycle followed by 5 s delayed neutron counting and a subsequent delay to fire the next neutron pulse). Assays require 30 min with a 10 min background count followed by 30 irradiation cycles. The time average neutron yield is 1E6 n/s.
- Measurement accuracy is similar to that of the Am(Li)-based AWCC assay.
- Measurement precision is equivalent to the traditional Am(Li)-based AWCC for ^{235}U masses below 200 g. However, as the mass value increases, the measurement precision degrades relative to the Am(Li) based measurement.
- The limiting factor in the performance of the DD/AWCC in this mode is the distance of the neutron target line to the end of the generator tube. It is not possible to place the MP320 close enough to the sample inside an AWCC to achieve the necessary neutron flux on the sample. A more compact generator would be required for this mode to achieve the performance of the Am(Li)-based AWCC.

Delayed Neutron Counting: High Repetition Rate Mode

- In high repetition rate mode, the neutron generator was operated at a pulse rate of 250 Hz, and delayed neutron counting is performed with millisecond duration time windows. Assays require 30 minutes which includes a10 minute background count followed by 300,000 irradiation cycles. The time average neutron yield is 2.2E6 n/s.
- The accuracy of this mode is similar to that of the Am(Li)-based AWCC measurement.
- The observed measurement precision is two times better than the traditional Am(Li)-based AWCC was obtained for the same total measurement times. Our results suggest additional improvement can be gained through further optimization of the counting time windows or use of a more compact neutron generator.
- Delayed neutron counting is somewhat more sensitive to the presence of ^{238}U because of its greater delayed neutron fraction compared to ^{235}U.
- Preliminary limited measurements with plutonium indicate the DD/AWCC can provide passive and active assay of plutonium. However, our initial measurements did not agree with the MCNP simulations. For example, the observed delayed neutron rate from 30 g of weapons-grade Pu was two times larger than the MCNP models predicted. The cause of this discrepancy has not yet been determined.

1. INTRODUCTION

International safeguards programs rely on active neutron interrogation techniques for accurate quantification of bulk uranium items. However, the neutron sources these techniques rely upon are either no longer available commercially or are too costly for routine safeguards application. In this work we examine the potential use of a commercial off-the-shelf (COTS) deuterium-deuterium (DD) neutron generator as an alternative neutron interrogation source for use in international safeguards. The Active Well Coincidence Counter (AWCC) (Menlove H. O., 1979) was selected for this study since it is the most commonly used active neutron system with a worldwide installed base of approximately 50 systems. This report examines the measurement performance and Monte Carlo N-Particle (MCNPX)-based (Pelowitz, 2008) investigation of an existing AWCC system modified to accept a single D-D neutron generator in place of the two Am(Li) neutron sources (McElroy, Cleveland, Croft, & Lousteau, 2016).

2. THE LARGE VOLUME-ACTIVE WELL COINCIDENCE COUNTER (LV-AWCC)

The AWCC (Menlove H. O., 1979) was developed to provide penetrating, accurate assay of bulk uranium-oxide samples, highly enriched uranium (HEU) metals and alloys, light water reactor fuel pellets and uranium-bearing scrap materials. The AWCC is a ^{3}He proportional tube–based neutron coincidence well counter where Am(Li) neutron sources located in the detector end-plugs provide a source of fast interrogating neutrons. The Am(Li) neutrons induce fission in the fissile materials contained within the item of interest. The fissile mass of the item is determined from the observed neutron coincidence rate using an empirically derived calibration curve. Although the Am(Li) neutron interrogation sources are no longer readily available, the AWCC can still serve as a versatile and high-performance neutron detector for international safeguards if the isotopic neutron sources are replaced with a pulsed neutron generator.

The LV-AWCC (Figure 1) is somewhat larger than the standard AWCC, but its design was simply scaled up from the standard unit and provides similar overall performance characteristics as shown in Table 1**Error! Reference source not found.**. Although the efficiency of the LV-AWCC is significantly higher than that of the AWCC, the AWCC outperforms the larger system due to a better source-sample coupling afforded by the smaller assay cavity.

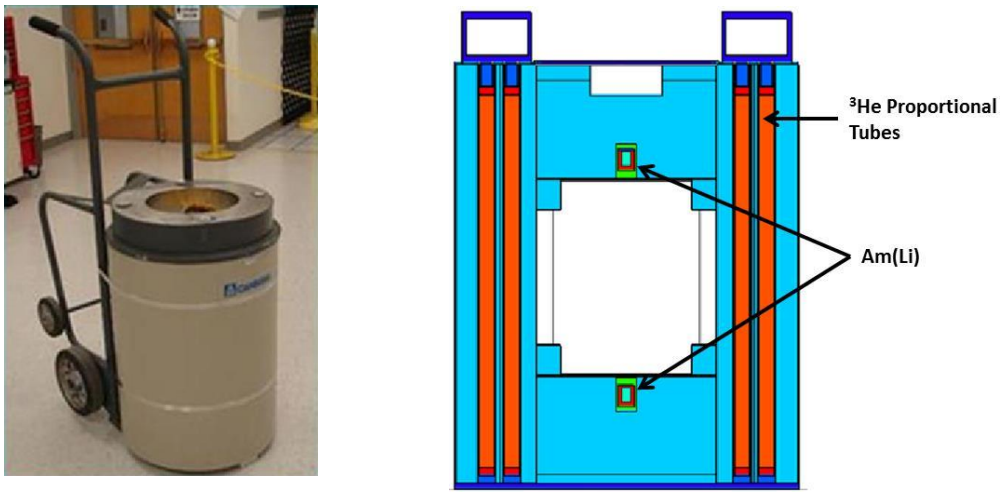

Figure 1. Photograph of the LV-AWCC (*left*) and a diagram of the LV-AWCC generated from the MCNPX input file (*right*). The LV-AWCC diagram has been adjusted to show the inner and outer ring of tubes, which are not normally visible at the same time in the vertical cross section through the counter.

Table 1. Comparison of AWCC and LV-AWCC characteristics

	AWCC	LV-AWCC
Assay cavity (ID × OD)	20.6 × 22.9 cm	37.4 × 28.0 cm
^{3}He proportional tubes		
Quantity	42 tubes	48 tubes
Active Length	50.8 cm	63.5 cm
Efficiency (bare ^{252}Cf at cavity center)	26.4%	30%
Die-away time	50 μs	54 μs
Sensitivity* (Doubles/g ^{235}U)	0.15	0.14
Precision# (200 g ^{235}U, 1,000 s, 1-σ)	8%	11%

* With a pair of 5E4 n/s Am(Li) sources configured in fast mode.
# Configured for fast mode, U_3O_8.

3. INTEGRATION OF THE D-D NEUTRON GENERATOR INTO THE LV-AWCC

Most neutron generators used in safeguards or waste assay applications are operated in a pulsed mode. Typical pulsed mode operation would create ~10 μs wide bursts of neutrons, which appear as coincident events to the AWCC (with 50 μs die-away time). To perform the active well coincidence measurement, the generator must be able to operate in a steady state (i.e., non-pulsed) mode. For the AWCC measurement, the generator must be able to provide a neutron yield between 4E4 and 1E7 n/s. This range provides the optimum measurement precision for uranium assay (accidentals limited), but without causing unacceptably large dead-time losses in a typical AWCC.

The D-D neutron generator was selected over the more common deuterium-tritium (D-T) generator to minimize the induced fission in ^{238}U. Although the 2.5 MeV neutrons from the D-D reaction and 14 MeV neutrons from the D-T reaction both exceed the fission threshold in ^{238}U, it is a much simpler task to minimize sensitivity to ^{238}U by the interrogation source if the lower energy D-D neutron generator is used. In addition, the lack of tritium simplifies shipping, and the lower neutron energy requires less additional shielding.

The D-D neutron generator selected for this evaluation is a ThermoFisher Scientific model MP 320 (Figure 2). The generator may be operated in steady state (non-pulsed) mode with a maximum yield of ~2.E6 n/s and average neutron energy of 2.48 MeV. Although not a small neutron generator tube by today's standard, the 12.1 cm diameter tube can be fit within the LV-AWCC or standard AWCC end-plugs. The principle drawbacks of the tube are its overall length (~56 cm) and location of the target line (i.e., point of neutron generation) ~14.4 cm from the end of the tube.

Figure 2. Photograph of the complete MP320 system (*left*) and the MP320 D-D neutron generator tube detached from the controller (*right*).

The modification to the LV-AWCC (Figure 3 and 4) positions the neutron generator tube through the bottom end-plug of the LV-AWCC such that the top of the generator is flush with the upper surface of the plug. The vertical position of the generator tube and the neutron production target line is a compromise between induced fission rate in ^{235}U, ^{238}U, and the detection efficiency of the D-D neutron source. The generator position and end-plug material selection are chosen to "minimize" the detection rate of the interrogating neutrons and the induced fission rate in ^{238}U, while maximizing the induced fission rate in ^{235}U. In our optimized design, the bottom end-plug is fabricated from high density polyethylene (HDPE). We found that replacing the HDPE top plug with a graphite plug improves the linearity of the fill height response and increases the overall fission rate within the sample.

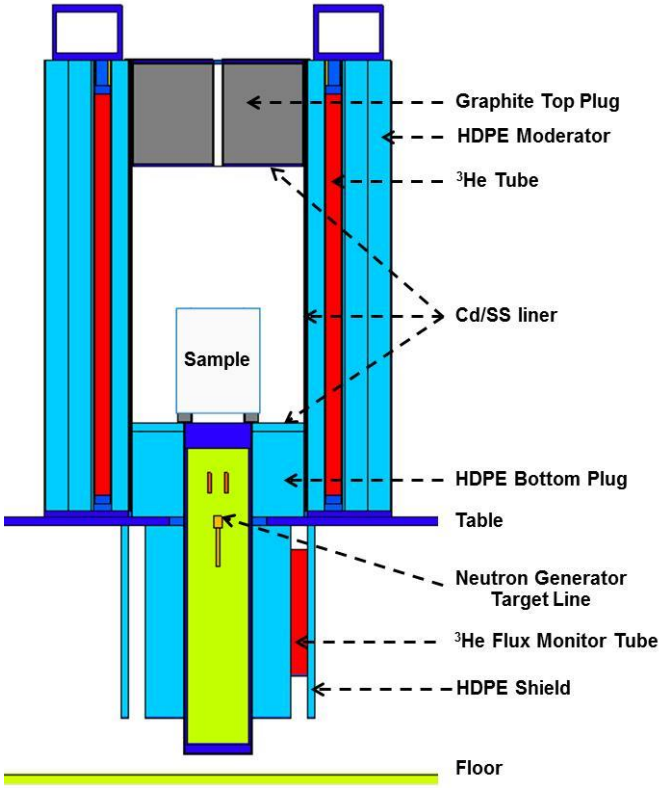

Figure 3. Rendering of the MCNP input file for the modified LV-AWCC. A shield and modified end-plug have been fitted to the LV-AWCC to accommodate the neutron generator.

For this study, the assay system was configured for "Fast Mode." That is, all surfaces of the assay cavity are lined with cadmium to minimize the impact of reentrant thermal neutrons on the induced fission rates.

The overall length of the MP320 generator tube required the LV-AWCC to be positioned on a 40 cm tall stand to allow proper placement of the generator within the counter. Although the overall neutron emission rate and exposure rate from the generator at full power do not pose a significant radiation safety risk, we opted to install an HDPE shield about the generator tube to minimize personnel exposure and potential interference from variable room backgrounds. A single small (20 cm active length) 1 atm ^{3}He tube is embedded into this shield to serve as a flux monitor to correct for variation in the neutron output from the generator.

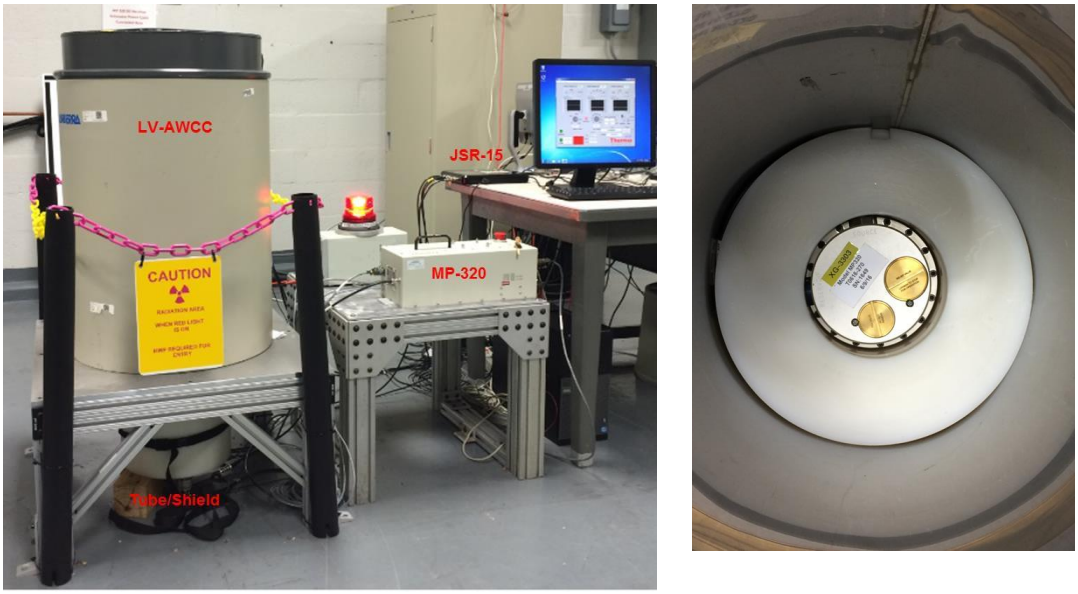

Figure 4. Photograph of the modified LV-AWCC with the neutron generator tube installed in the bottom end-plug. The photo on the right shows the top of the neutron generator tube mounted in the bottom HDPE end-plug inside the AWCC with the Cd liner removed.

Radiation Safety

The maximum exposure rate observed inside the assay cavity was 20 mR/h while operating at a neutron yield of 2E6 n/s. Outside the assay cavity the exposure rate was less than 0.5 mR/h. For this short-term project, an interlock switch was not installed on the top plug thus requiring that the system be posted to prevent personnel from inadvertently removing the top plug while the system is in operation. At ORNL the posting is not be required if an appropriate interlock is installed.

3.1 DATA ACQUISITION CONFIGURATION

The data acquisition system is based on COTS components. The active coincidence counting measurement uses the same acquisition electronics and data acquisition software currently used by the International Atomic Energy Agency (IAEA) with the standard AWCC measurement. The delayed neutron counting data is acquired using a standard Multi-Channel Scaler (MCS) module and acquisition software also in routine use by the IAEA for safeguards measurements. Due to the variability of the neutron generator yield, a flux monitor was added. In this case, the flux monitor is a single 8 in. active length, 1 atm partial pressure ^{3}He tube mounted in the HDPE shield below the AWCC. The output of the

flux monitor is read using the shift register AUX scaler input. The acquisition modules used in the DD-AWCC testing are listed here, and a block diagram of the configuration is shown in Figure 5.

Data Acquisition Modules

- **Shift register:** JSR-15 handheld multiplicity shift register (HHMR) available from Canberra Industries
- **Multi-Channel Scaler:** LYNX digital signal processor (DSP) available from Canberra Industries

Coincidence counter

- Standard Canberra Industries junction box design utilizing eight (8) JAB-01
- Amplifier\preamplifier\discriminator boards with an internal derandomizer board

  Inputs
  - **LVPS in:** +5V @ <0.5 Amps, supplied using a COTS adjustable power supply
  - **HV bias in:** +1,690 V supplied by JSR-15

  Outputs
  - **Sum signal:** Derandomized sum of all 8 detector banks and fed to the Signal input of the JSR-15
  - **Inner ring:** Derandomized sum of the four inner ring detector banks and fed to Aux 1 input of JSR-15
  - **Outer ring:** Not used for these measurements

Flux Monitor

- **^{3}He tube:** TGM, 1 in. OD, 8 in. active length, 1 atm. ^{3}He partial pressure
- **Pre-amplifier/amplifier/discriminator module:** Precision Data Technologies PDT 110A
  - **LV in:** +5V @ <0.1 Amps, supplied from the JSR-15
  - **HV bias in:** supplied by the JSR-15
  - **TTL Out:** Fed to the AUX 2 input of the JSR-15

Software

- **Coincidence counting software:** IAEA Neutron Coincidence Counting (INCC) Ver. 5.1.12
- **Delayed-neutron data acquisition:** Canberra Genie 2000, Ver. 3.3

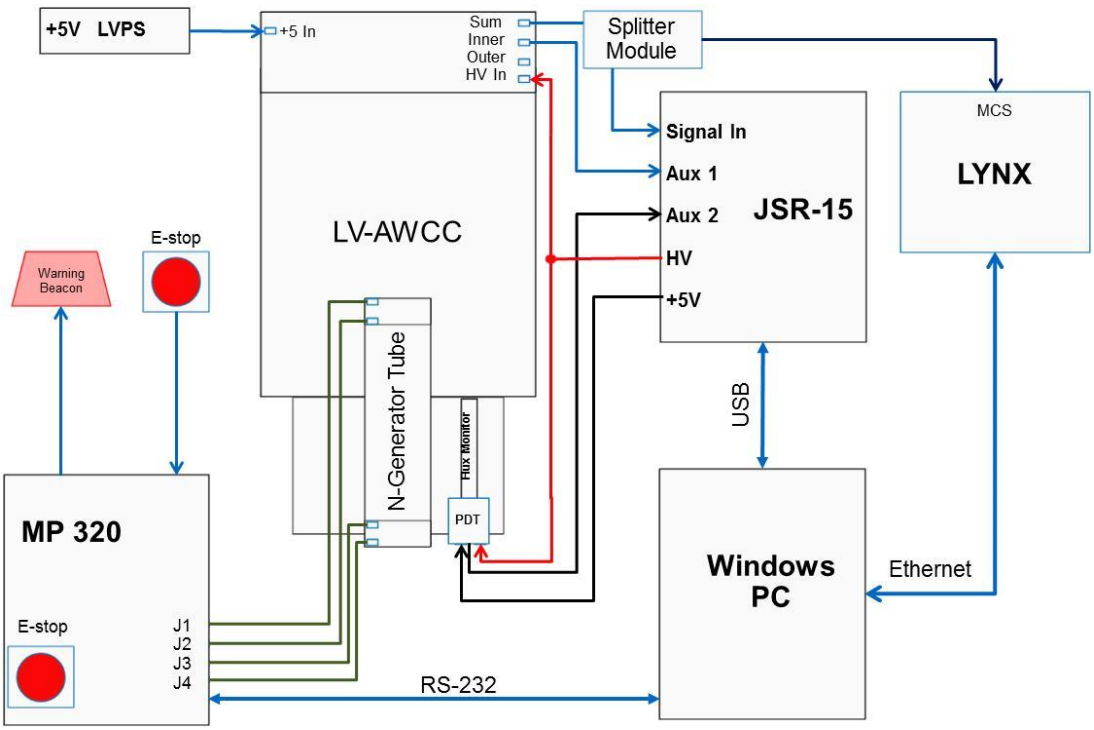

Figure 5. Diagram showing the electronics configuration for the DD-AWCC testing.

4. PERFORMANCE OF THE INTEGRATED D-D GENERATOR/AWCC

To examine the expected performance of the integrated D-D generator and LV-AWCC, hereafter referred to as the DD/AWCC, a series of MCNPX simulations were performed followed by a series of measurements of DU, LEU, HEU, and ^{233}U items.

4.1 SIMULATED RESPONSE

The MCNPX-based simulations examined the response as a function of mass, density, and enrichment for a variety of sample containers.

4.1.1 Coincidence Counting: Basic Response Profile

The response profile for the DD/AWCC was examined by simulating the response from a series of 93% enriched U_3O_8 oxide containers. For this first series, the density was fixed at 3.5 g/cc, while the fill height was systematically increased. The coincidence count rates were determined for a neutron generator yield of 2.28E5 n/s, which was selected to provide similar coincidence rates to those observed from the Am(Li)-based AWCC measurements. The resulting response function (Figure 6) was found to be well represented by a power function of the ^{235}U mass.

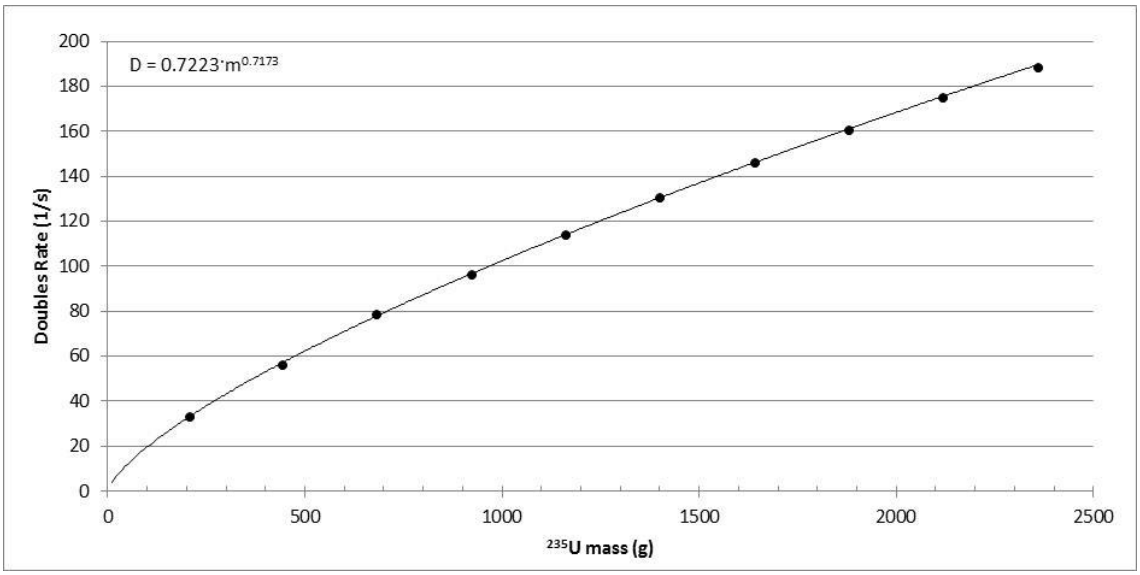

Figure 6. Plot of the simulated coincidence rates for a series of U_3O_8 samples of 93% enriched uranium as a function of ^{235}U mass from the LV-AWCC system with D-D neutron interrogating source (2E5 n/s interrogation rate). Note: the error bars due to MCNPX simulations are too small to be visible in this plot.

4.1.2 Coincidence Counting: Enrichment Effect

The higher energy of the D-D neutron compared with the Am(Li) neutron average energy, suggests the DD/AWCC should be more sensitive to the presence of ^{238}U. To investigate this enrichment effect, a second series of simulations were performed for uranium enrichments of 4.5%, 20%, and 50%. The same container parameters defined in the preceding section were input, and the fill height increased in the same fashion. Figure 7 shows the expected coincidence rates from this series of simulated assays of U_3O_8 oxide containers. The results indicate that an enrichment dependence is expected using the D-D generator; however, the impact is only significant for enrichments below 50%.

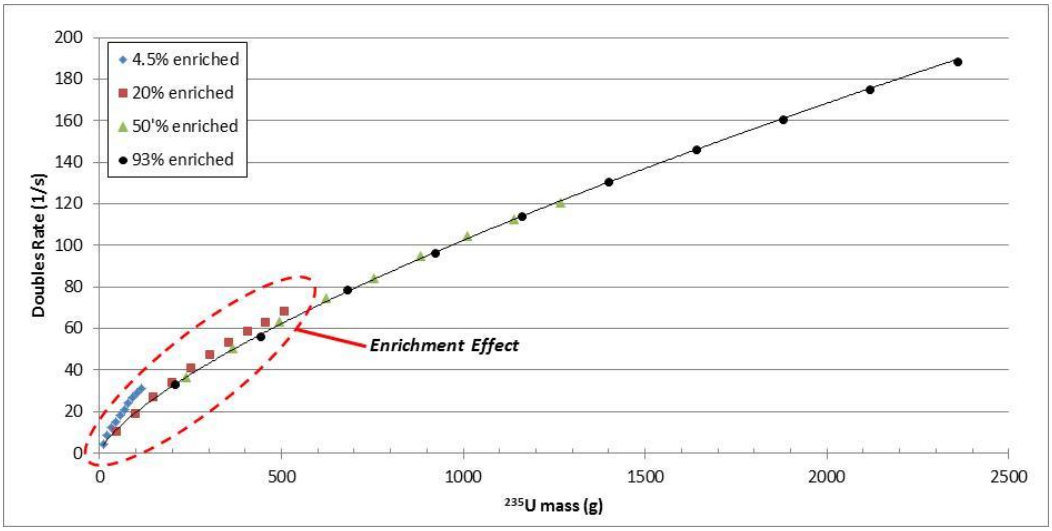

Figure 7. Plot of the simulated coincidence rates for a series of U_3O_8 samples of various enrichments as a function of ^{235}U mass from the LV-AWCC system with D-D neutron interrogating source (2E5 n/s interrogation rate). The error bars resulting from the MCNPX simulations are too small to be visible in this plot.

Analysis of the data suggests a simple correction is required based on a ^{235}U effective mass analogous to the ^{240}Pu effective mass used in passive neutron coincidence counting except that the conversion factors between ^{235}U and ^{238}U must be determined through simulation or calibration. We find the following simple relation works well across all test cases considered for a given counter arrangement and container size:

$$m_{235_{eff}} = m_{235} + f \cdot m_{238} ,$$

where $m_{235_{eff}}$ is the ^{235}U effective mass,
m_{235} is the ^{235}U mass,
m_{238} is the ^{238}U mass, and
f is an empirically determined conversion factor.

For the test cases considered for the selected system configuration, we find from the simulations that $f = 0.039$ for the active coincidence counting mode using the D-D generator. The data from Figure 7 is replotted in Figure 8 against $m_{235_{eff}}$ and, as can be seen, the entire data set is well represented by a single calibration curve (in this case a simple power function). The enrichment must be known or measured to apply this correction; however, in practice, a representative calibration over a narrow range of enrichments can also be applied.

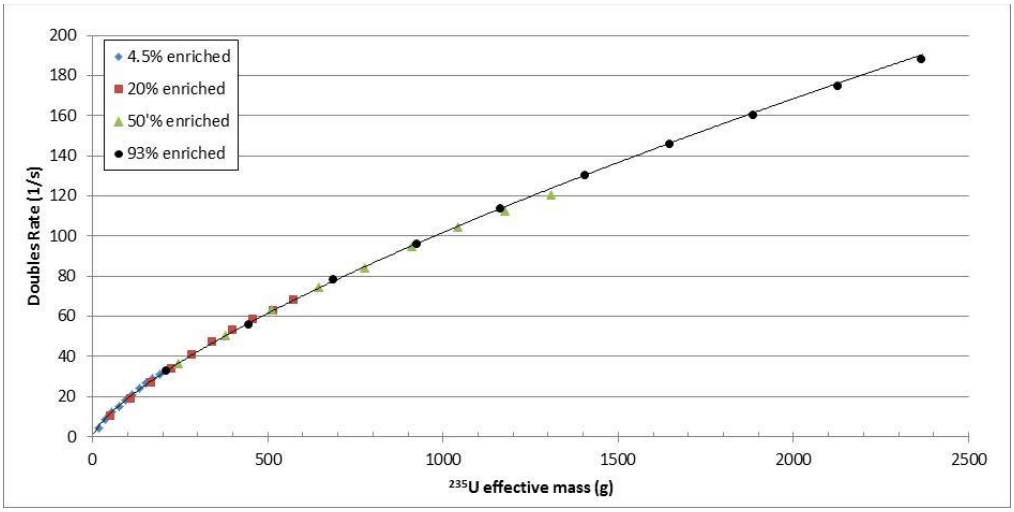

Figure 8. Plot of the simulated coincidence rates for a series of U_3O_8 samples of various enrichments as a function of ^{235}U effective mass from the LV-AWCC system with D-D neutron interrogating source (2E5 n/s interrogation rate).

4.1.3 Coincidence Counting: Density Effect

The impact of the bulk density of the uranium was examined by simulating the coincidence response from a series of containers with varying fill heights and densities. A plot of the resulting response is shown in Figure 9 and suggests a dependence on sample density. The maximum impact of the density effect is on the order of a few percent and can be accommodated by calibrations using representative standards, which is traditionally done for the AWCC. However, this dependence seems better characterized in terms of fill height. The traditional AWCC utilizes two Am(Li) sources to provide a more uniform spatial response within the assay cavity. The D-D generator affords only a single source of interrogating neutrons leading to a more pronounced vertical response profile such that the induced fission rate decreases as a function of height.

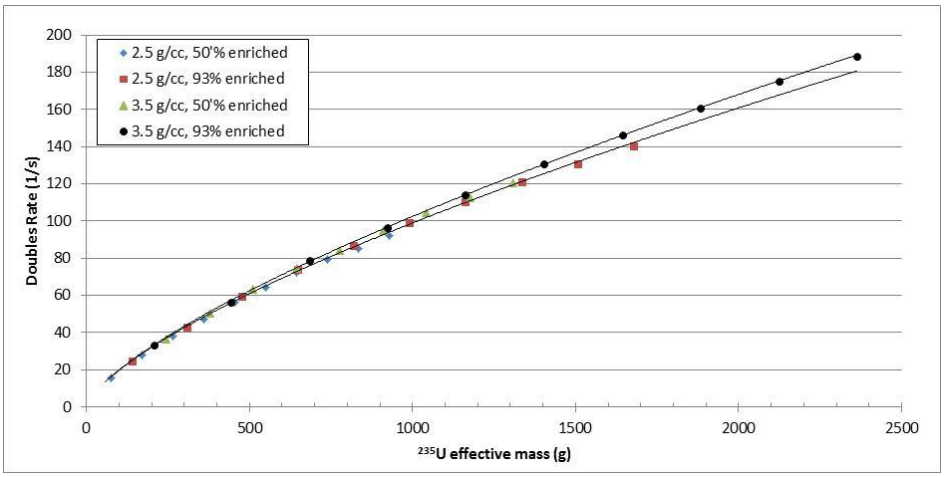

Figure 9. Plot of the simulated coincidence rates for a series of U_3O_8 samples of various enrichments as a function of ^{235}U mass from the LV-AWCC system with D-D neutron interrogating source (2E5 n/s interrogation rate).

The vertical response profile for the DD/AWCC was examined by simulating the response from a 5 cm tall uranium disc as a function of height above the floor of the assay cavity. The results are shown in Figure 10, and a similar plot for the standard AWCC is provided in Figure 11 for comparison. The response from a container of uranium is an average over the extent of the material within the container so that the impact of the fill height is much less pronounced than suggested in Figure 10. For example, the expected difference in the doubles rate across the mass range 0–2000 g ^{235}U for densities of 2.5 g/cc compared with a 3.5 g/cc sample is less than 2.5%.

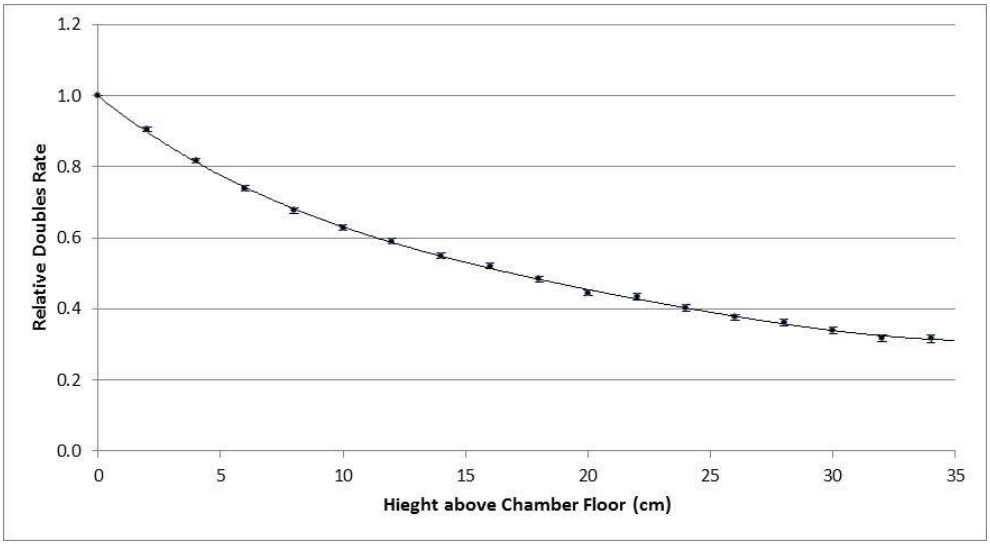

Figure 10. Plot of the simulated coincidence rates for a 5 cm tall U_3O_8 sample as a function of height above the DD/AWCC assay cavity floor.

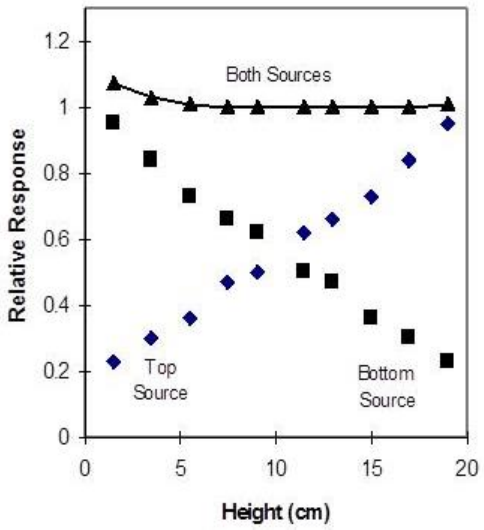

Figure 11. Plot of the measured coincidence rates for a 5 cm tall U_3O_8 sample as a function of height above the standard AWCC assay cavity floor (Menlove H. O., 1979).

4.1.4 Coincidence Counting: Measurement Precision (MCNP Simulations)

While the linearity of the DD/AWCC method equals or exceeds that obtained using the Am(Li)-based source interrogation, the measurement precision is degraded using this approach. Figure 12 presents the estimated measurement precision in the doubles rate as a function of $^{235}U_{effective}$ mass, and the estimated measurement precision in the mass assay result is presented in Figure 13. The measurement precision is generally two times poorer than the Am(Li)-based measurement. This is a result of the poorer source coupling and less effective shielding of the detectors from the D-D neutrons. By chance, in our model, D-D neutrons emitted at the target line position have the same detection efficiency for the interrogating neutrons as the Am(Li) neutrons in the AWCC configuration. That is, the totals rate from the interrogating neutron flux alone is approximately 7000 cps for both AWCC and DD/AWCC configurations given a 100,000 n/s source term. However, in this location, the induced fission rate is lower by a factor of 2 than obtained using the Am(Li) sources. This apparent limitation could be overcome by using a more compact generator.

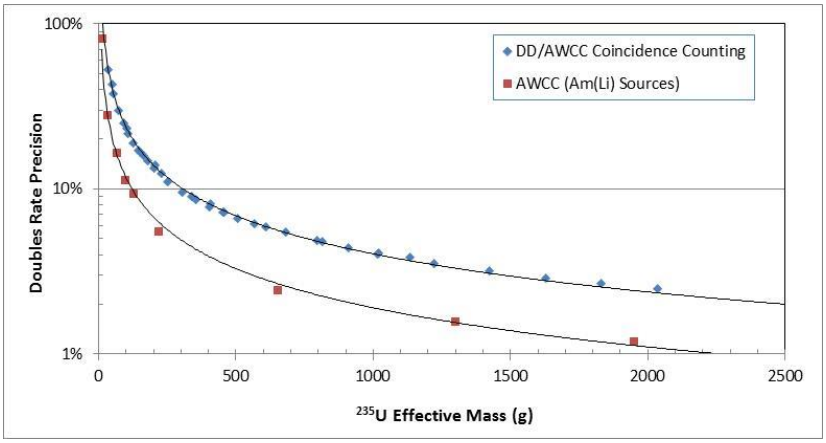

Figure 12. Expected measurement precision in the doubles rates for the LV-AWCC operated with Am(Li) or D-D neutron interrogation source for a 1200 s active assay in fast mode.

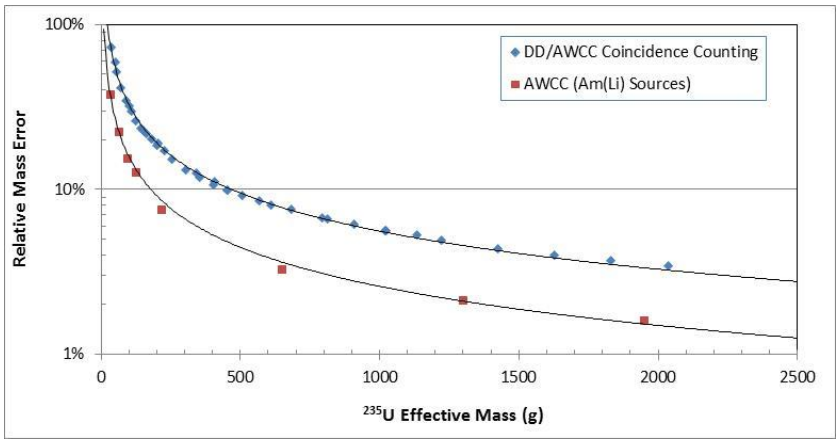

Figure 13. Expected measurement precision in the reported mass values for the LV-AWCC operated with Am(Li) or D-D neutron interrogation source for a 1200 s active assay in fast mode.

4.2 AVAILABLE URANIUM TEST ITEMS

The uranium items available for characterization of the DD/AWCC performance are listed in Table 2.

Table 2. Uranium items available for the characterization of the DD/AWCC measurement performance

ID	Material form	Geometry	Type	Uranium mass (g)
JANY	U metal	Cylindrical shell	DU (0.2%)	8,000
JAPO	U metal	Cylindrical shell	DU (0.2%)	18,000
DU5852	U metal	Spherical shell	DU (0.2%)	937
YST-1-B	U metal	Solid sphere	DU (0.2%)	1,000
NBS-071-078	U_3O_8	Right cylinder	U-natural (0.7%)	169
NBS-071-045	U_3O_8	Right cylinder	LEU (4.5%)	169
NBL-001	U_3O_8	Right cylinder	HEU (20%)	195
NBL-002	U_3O_8	Right cylinder	HEU (52%)	195

NBL-003	U_3O_8	Right cylinder	HEU (93%)	195
U233-1	U metal/oxide	Cylindrical-distributed	^{233}U (100%)	13.2
U233-2	U oxide/pellets	Cylindrical-distributed	^{233}U (100%)	63.0

4.3 DD/AWCC COINCIDENCE MEASUREMENTS

The active coincidence measurement using the D-D neutron generator does not require the use of multi-channel scaling. The measurement is performed using only the JSR-15 shift register. Because the LV-AWCC includes eight amplifier discriminator boards plus an internal derandomizer board, the current draw exceeds the 500 mA limitation of the JSR-15, which requires the use of an external +5V low-voltage power supply (LVPS). The flux monitor is used to monitor and correct for variations in the neutron output from the neutron generator. Both the JSR-15 and MP320 are controlled from the same Windows-based computer. Data is acquired using the INCC software while the flux monitor correction is performed offline after completion of the measurement.

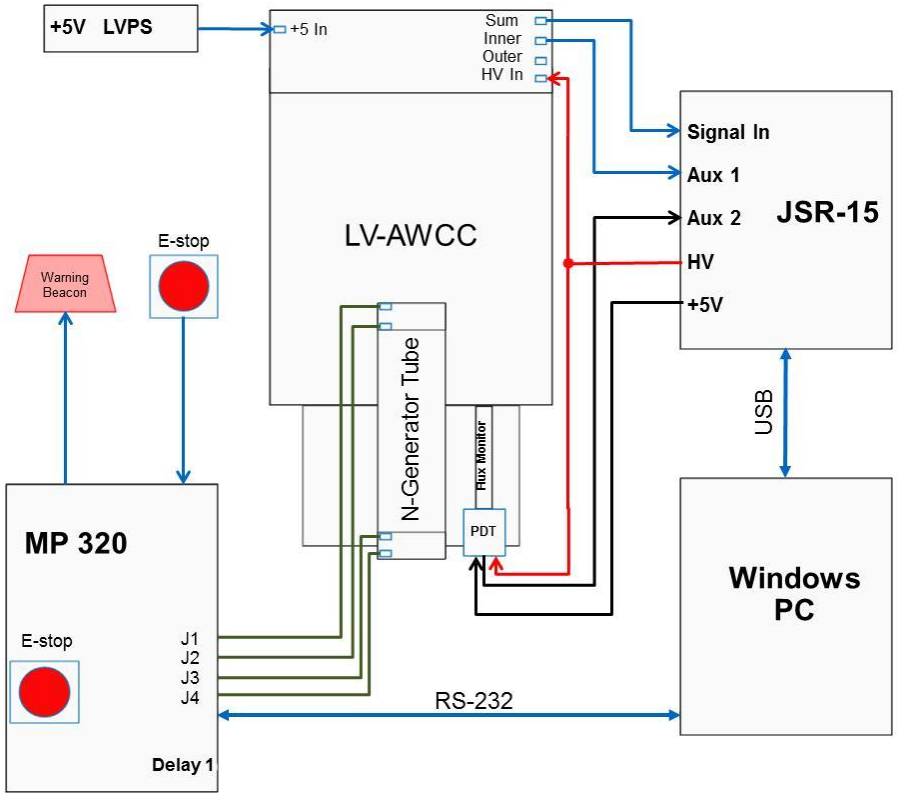

Figure 14. Diagram showing the electronics configuration for the DD-AWCC for simple active coincidence counting.

4.3.1 Interrogating Neutron Yield

For the active coincidence measurements, the MP320 neutron generator is operated in steady state mode (i.e., 100% duty factor). The measurement precision of the AWCC is almost independent of the interrogating neutron source strength for uranium oxides and metals once a threshold source strength is reached. Arbitrarily, we opted for neutron generator settings that would provide approximately the same doubles rate for the 93% enriched NBL003 standard as measured using the 100,000 n/s Am(Li) sources. The resulting settings, 30 µA beam current and 50 kV high voltage, yield a singles rate of approximately

17,100 cps for the empty cavity. The MCNP simulations predict a detection efficiency of 7.5% for neutrons emitted from the generator target line. From this, the estimated D-D neutron yield is 2.28E5 n/s.

4.3.2 Neutron Generator Output Stability and Normalization

The neutron yield from this (or any other) neutron generator is expected to vary throughout the day and from day-to-day depending on its usage and how the tube ages. Over the course of 2 months of measurements we observed that the neutron output tended to fluctuate about ±0.5% over the course of a day. To correct for the variation in neutron yield, a single, short, low pressure ^{3}He tube was installed into the HDPE shield surrounding the neutron generator to monitor and correct for these variations. All active coincidence measurements will be corrected based on the ratio of the measured flux monitor relative to an essentially arbitrary reference rate of 460 cps (although, 460 cps was the first measured flux monitor rate for the chosen beam current and HV settings).

Table 3 provides the generator settings and observed count rates for a series of measurements on the DU item JANY. Nine measurements were performed for this standard. Two of these measurements were performed with significantly different interrogating neutron strengths while the count rate variations in the remaining seven measurements are caused by the normal fluctuations in the generator output.

Table 3. Active count rates for the uranium standard JANY obtained using the DD/AWCC in coincidence counting mode

Assay time(s)	Generator settings	Singles rate (cps)	Doubles rate (cps)	Inner ring rate (cps)	Flux monitor Rate (cps)
1800	60 µA; 60 kV	63988.26 ± 30.93	281.96 ± 15.64	40238.60 ± 19.66	1747.02 ± 1.29
1800	60 µA; 60 kV	63771.79 ± 21.32	274.97 ± 16.94	40110.85 ± 13.44	1738.50 ± 1.27
3600	30 µA; 50 kV	16902.81 ± 2.49	80.64 ± 3.43	10704.40 ± 1.92	461.57 ± 0.35
3600	30 µA; 50 kV	16973.61 ± 2.28	72.42 ± 2.95	10753.77 ± 1.67	463.03 ± 0.35
3600	30 µA; 50 kV	17243.47 ± 3.63	76.55 ± 2.29	10927.90 ± 2.51	469.54 ± 0.37
3600	30 µA; 50 kV	17228.00 ± 2.44	76.49 ± 2.24	10917.32 ± 1.84	469.21 ± 0.37
3600	30 µA; 50 kV	17252.31 ± 2.54	76.79 ± 2.49	10933.03 ± 1.81	470.14 ± 0.35
3600	30 µA; 50 kV	17238.96 ± 2.46	78.10 ± 2.40	10922.55 ± 1.71	470.36 ± 0.38
3600	30 µA; 50 kV	17319.27 ± 3.18	76.72 ± 2.27	10974.84 ± 2.35	472.33 ± 0.39

The effectiveness of the flux monitor normalization is illustrated in Table 4. The flux monitor normalization factor (referenced to an arbitrary value of 460 cps) is used to correct for fluctuations in the generator yield due to normal variations or deliberate changes in generator settings (e.g., increased output to overcome a large (α, n) emission rate from the sample). Without the normalization the routine fluctuation of the neutron yield (as evidenced by the variations in singles rates) is approximately 0.8% from assay to assay, applying the normalization reduces this fluctuation to 0.1% and has insignificant impact on the measurement uncertainty. The flux monitor correction appears to be less effective for the inner ring rate only because the INCC software does not apply a dead-time correction to the Scaler inputs.

Table 4. Flux monitor normalized rates for the uranium standard JANY

Flux monitor normalization	Singles rate	Doubles rate	Inner ring rate
3.798 ± 0.003	16,848.43 ± 8.14	74.24 ± 4.12	10,595.03 ± 5.18
3.779 ± 0.003	16,873.72 ± 5.64	72.76 ± 4.48	10,613.14 ± 3.56

1.003	± 0.001	16,845.21	± 2.48	80.36	± 3.42	10,667.92	± 1.92
1.007	± 0.001	16,862.50	± 2.27	71.94	± 2.93	10,683.37	± 1.66
1.021	± 0.001	16,893.26	± 3.56	74.99	± 2.24	10,705.96	± 2.46
1.020	± 0.001	16,890.02	± 2.40	74.99	± 2.19	10,703.14	± 1.80
1.022	± 0.001	16,880.24	± 2.48	75.14	± 2.44	10,697.25	± 1.77
1.023	± 0.001	16,859.19	± 2.41	76.38	± 2.35	10,681.93	± 1.68
1.027	± 0.001	16,867.01	± 3.09	74.72	± 2.21	10,688.26	± 2.29
Average		16,868.84		75.06		10,670.67	
Standard deviation		16.99		2.39		39.75	
Standard deviation (%)		0.10%		3.18%		0.37%	

4.3.3 DD/AWCC Active Coincidence Results

Additional active coincidence measurements using the D-D generator were performed on several HEU, LEU, and DU objects. Multiple measurements were performed on several of the items to obtain improved statistics as time available with each item permitted. The weighted average singles and doubles rates for these items are provided in Table 5. The single and doubles uncertainties shown are based on this weighted averaging. The table also provides the typical measurement precision obtained for a 1 h total measurement time for each of the items, and the 3,600 s precision value represents the typical measurement precision for a 1 h count time. For active coincidence counting with the D-D generator, the ^{235}U effective conversion factor for ^{238}U determined from the MCNP simulations is 0.039 g ^{235}U/g^{238}U. The ^{235}U effective mass provided in Table 5 is determined using this conversion factor.

Table 5. Flux monitor normalized rates for the uranium test items

	U mass (g)	^{235}U Enrich.	^{235}U effective mass (g)	Assays	Singles rate		Doubles rate		Precision (3600 s)
EMPTY	0	—	0.0	5	17,104.68	± 5.41	2.86	± 0.89	69%
U233-1	13.2	—	9.5	6	17,026.22	± 5.84	7.24	± 1.38	41%
U233-2	63.0	—	16.5	8	16,998.57	± 3.75	14.31	± 0.97	47%
NBS·071·078	169	0.7%	48.0	3	17,071.72	± 7.88	5.68	± 1.34	52%
NBL001	195	20%	78.8	2	17,054.35	± 9.32	10.33	± 1.62	19%
NBL002	195	52%	46.7	2	17,091.88	± 7.69	17.62	± 1.28	22%
NBL003	195	93%	106.8	4	17,156.67	± 6.63	23.84	± 1.20	10%
DU 5852	937	0.2%	182.0	3	17,017.98	± 7.46	6.84	± 2.05	10%
JAPO	8,000	0.2%	409.6	5	16,822.57	± 6.10	45.55	± 1.21	6%
JANY	18,000	0.2%	921.7	9	16,869.05	± 4.52	75.12	± 0.89	4%

Although from the MCNP simulations we expect to see fill height and possibly density effects on the measured count rates, we have plotted the measured coincidence rates as a function of ^{235}U effective mass in Figure 15. The resulting response was found to be a well behaved function of the ^{235}U effective mass. A quadratic was fit to the measured values to obtain a response function that can then be used to estimate the uncertainty in the mass assay results. A very obvious feature of the plot is a significant positive bias at 0 mass equal to 2.9 cps. This active coincidence background has not yet been explained, but it has proven to be reproducible for the selected neutron generator settings. Since this active background was not

reproduced in the MCNP simulations, it is assumed that it is electronic in origin (e.g., a low level of double pulsing).

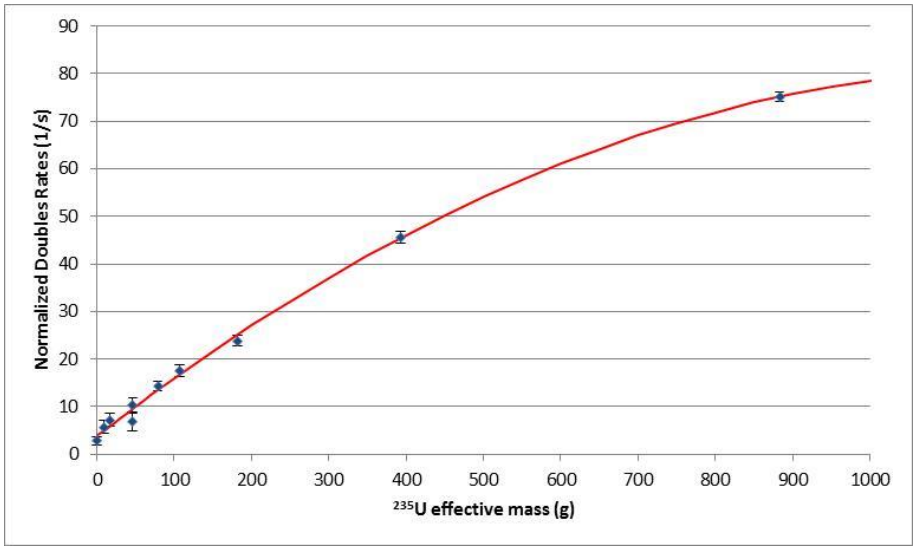

Figure 15. Measured DD/AWCC doubles rate as a function of ^{235}U effective mass. The red line represents a quadratic response fit to the data.

The relative measurement precision determined from the MCNP simulations is compared to the measured precision in Figure 16. The 2.9 cps active coincidence background is stripped off before calculating the relative measured precision to provide a more reliable indication of the measurement performance. From the plot we can see that the MCNP simulation provide an accurate estimate of the measurement precision.

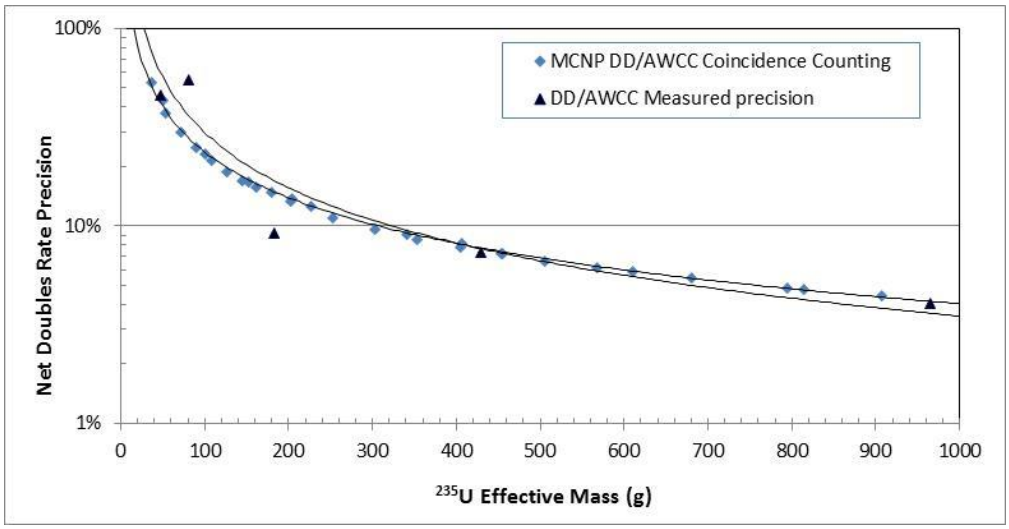

Figure 16. Comparison of the measured and predicted net DD/AWCC doubles rate precision as a function of ^{235}U effective mass (3600 s assay time). The constant 2.9 cps coincident background was subtracted before calculating the measured precision.

5. DELAYED NEUTRON COUNTING

An alternative active neutron assay methodology to the AWCC approach is delayed neutron counting such as the ^{252}Cf shuffler (Rinard P. M., 1991).* The ^{252}Cf shuffler is among the most accurate non-destructive assay techniques available to safeguards and material control and accountability programs with precision and accuracy of 0.1 to 0.3% achievable. However, the large footprint, mechanical complexity, and relatively high cost resulted in limited deployment of the systems. The DD/AWCC system allows this delayed neutron based measurement technique to be applied in a more cost-effective and practical manner.

The shufflers introduce a large (typically 1E8 to 1E9 n/s) ^{252}Cf source into the assay cavity via a mechanical drive. The ^{252}Cf neutrons induce fission within the item of interest, the source is then removed, and the delayed neutrons emitted following the fission events are counted. The sequence of irradiation followed by delayed neutron counting is repeated until the desired measurement precision is achieved.

The ^{252}Cf shuffler active interrogation cycle is divided into four time intervals.

- Forward travel time, t_f, the time required to transfer the source from its storage location to the irradiation position
- Irradiation time, t_{irr}, the time the ^{252}Cf source is located at the irradiation position
- Reverse travel time, t_{rev}, the time required to transfer the source back to the storage location
- Delayed neutron counting time, t_{dn}, time interval available to count delayed neutrons.

The total cycle time, t_{tot}, is the sum of these times.

$$t_{tot} = t_f + t_{irr} + t_{dn} + t_{rev}$$

Figure 17 shows the total neutron count rate composition for a single interrogation/counting cycle of the shuffler assay while Figure 18 illustrates the build-up of the delayed neutron precursors over successive interrogation cycles. With the ^{252}Cf source in the assay cavity, the delayed neutron precursors build-up, and the shortest lived groups will saturate during the irradiation interval. However, the interrogating source overwhelms the delayed neutron signal while the generator is firing, so the delayed neutron precursors are counted in the low background environment afforded by storing the source. When the source is retracted, the delayed neutron emission can be measured during a period of low background, providing significantly better sensitivity than the Am(Li)-based AWCC measurements.

* We would like to acknowledge the previous work by Schear and Tobin [23] examined the potential to adapt the ^{252}Cf drum shuffler for use with a D-T neutron generator. Their work focused on replacement of the interrogating source in an existing large-scale ^{252}Cf system. Here we examine the potential to add the capability of the shuffler technique to the portable neutron coincidence well counters, such as the AWCC.

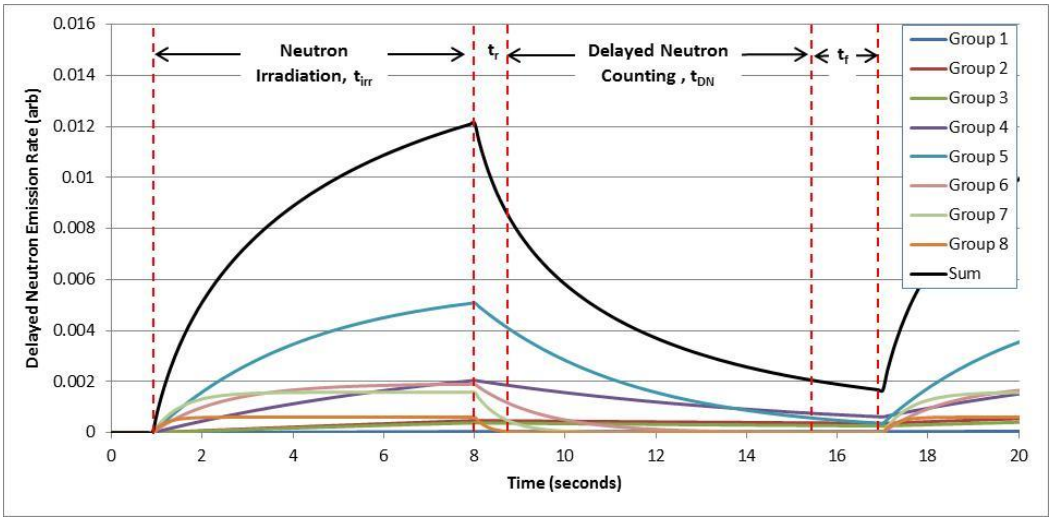

Figure 17. Build-up and decay of the 8 group delayed neutron populations within the ^{252}Cf shuffler as a function of time during the initial interrogation cycle (shuffle).

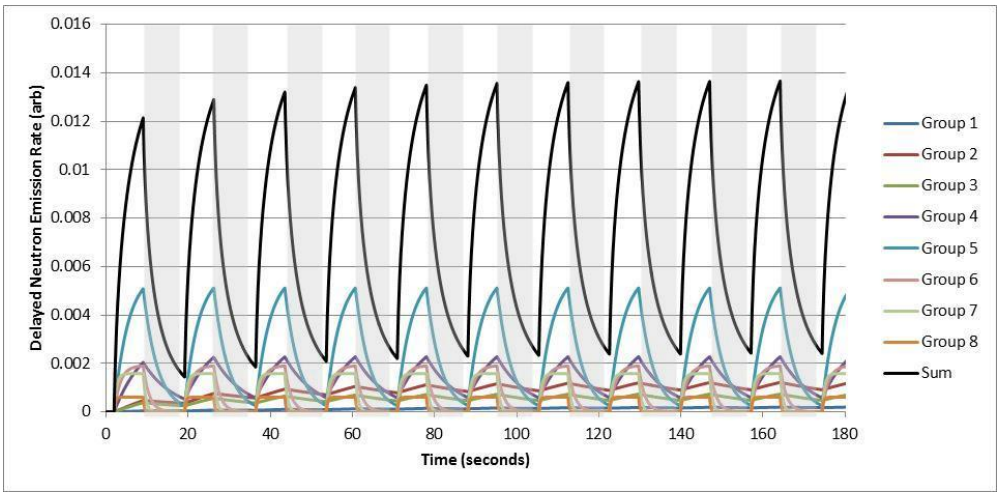

Figure 18. Buildup and decay of the 8 group delayed neutron populations within the ^{252}Cf Shuffler as a function of time. The shaded regions represent the delayed neutron counting windows (the interrogating neutron flux is not shown). A typical assay would include 34 interrogation cycles each with alternating 7 s interrogation and 7 s delayed neutron counting windows.

Figure 19 shows the measured counts versus time from the assay of a large uranium item in the ^{252}Cf shuffler summed over each of the interrogation cycles. The lack of sharp edges to the interrogation pulse is due to the 1 s source movement time from assay cavity to the storage module. The exponential decay of the delayed neutron emission rate can be seen in the plot. The delayed neutron response function is given in terms of the average delayed neutron count rate. The counts in each of the delayed neutron windows following each irradiation are summed and then divided by the sum of the times the window is open. For the mechanical source drive used with the ^{252}Cf shuffler it has been necessary to apply a cycle-by-cycle correction to the observed count rates to adjust for the slight differences in timing for each shuffle. However, the pulsing of the neutron generators is more reproducible, and it is only necessary to adjust the count rates for the number of cycles per each assay.

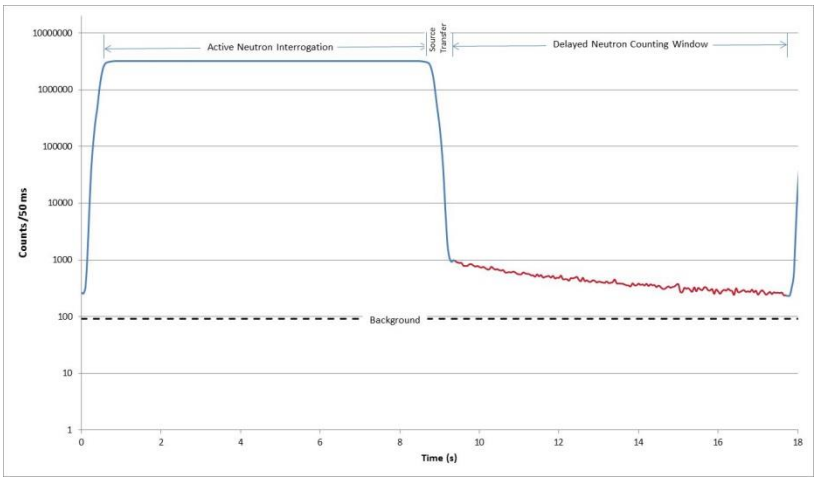

Figure 19. Measured ^{252}Cf shuffler neutron interrogation and delayed neutron counting cycle (equivalent interrogating ^{252}Cf source strength ~7E8 n/s, equivalent ^{235}U mass 5 kg). The dotted line represents the passive neutron count rate (background) from the item.

5.1 DELAYED NEUTRON COUNTING USING THE D-D NEUTRON GENERATOR

Integration of the D-D neutron generator into the LV-AWCC provides a means for implementation of a compact shuffler assay system. Rather than using a mechanical mechanism to shuttle a ^{252}Cf source into and out of the assay cavity, the neutron generator may be turned on and off, replicating the shuffler's alternating irradiation and delayed neutron count sequence. Since the average spontaneous neutron energy of ^{252}Cf (2.1 MeV) and emitted D-D neutrons (2.48 MeV) are little different from each other, the system response to the two neutron sources are expected to be very similar. To provide an equivalent interrogation sequence to that of the ^{252}Cf shuffler, the neutron generator is fired for several seconds to provide the interrogating neutron flux, then it is shut off for several seconds to allow for counting of delayed neutrons and the cycle repeated.

In the course of this study we examined three different operating modes of the MP320 generator for the delayed neutron measurement. These modes are described as follows:

- Slow Pulse mode: An integral mode of the MP320 that allows the generator to be cycled on and off cleanly and quickly on time scales of seconds to minutes. In principle, this mode most closely matches the historical assay sequence of the ^{252}Cf shufflers (e.g., 7 s irradiation followed immediately by 7 s delayed neutron counting). Unfortunately, it seems that the MP320 cannot tolerate prolonged operation in this mode and doing so is expected to dramatically shorten the life of the neutron generator tube.

- Cycled steady state mode: In this mode the operation of the MP320 is controlled by a simple external software code where the generator set for steady state operation is turned on using a time consuming "soft start" protocol that introduces less stress on neutron generator tube. However, this mode does not provide a clean start to neutron production, and the minimum cycle time is limited by the internal firmware of the MP320 controller (approximately 37.5 s).

- High frequency pulse mode: In this mode, the MP320 fires periodically, providing a sharp rise and fall (i.e., the ramp up and ramp down time) to the neutron production. However, the minimum frequency or repetition rate for the MP320 is 250 Hz, limiting the irradiation and delayed neutron counting time per cycle to millisecond time scales.

While the first two modes, slow pulse and cycled steady state, more closely replicate the traditional ^{252}Cf shuffler irradiation and delayed neutron counting sequences, the fast pulse mode will be shown to provide significantly improved measurement precision compared with the first two modes and with the Am(Li) source–based coincidence counting mode.

5.2 DELAYED NEUTRON COUNTING: MP320 SLOW PULSE MODE

The original intention for this measurement was to operate the MP320 in its "Slow Pulse" mode (also referred to as its "Standby mode"), which allows the generator to be cycled on and then off repeatedly and rapidly for predefined periods of time. However, unlike the standard pulse mode which cycles on the order of milliseconds (250 to 10,000 Hz), this mode operates on the order of seconds to minutes. In this mode, the generator is set to operate in a steady state mode producing neutrons for a preset number of seconds. At the end of the irradiation period, neutron production is halted but the HV supplies are not turned off, allowing rapid restart of neutron production when called on to do so. Figure 20 shows a measured count rate from the DD/AWCC as a function of time with the MP320 operating in Slow Pulse mode. In this mode the neutron production rise time is on the order of 1 s, and neutron production ceases within a few microseconds.

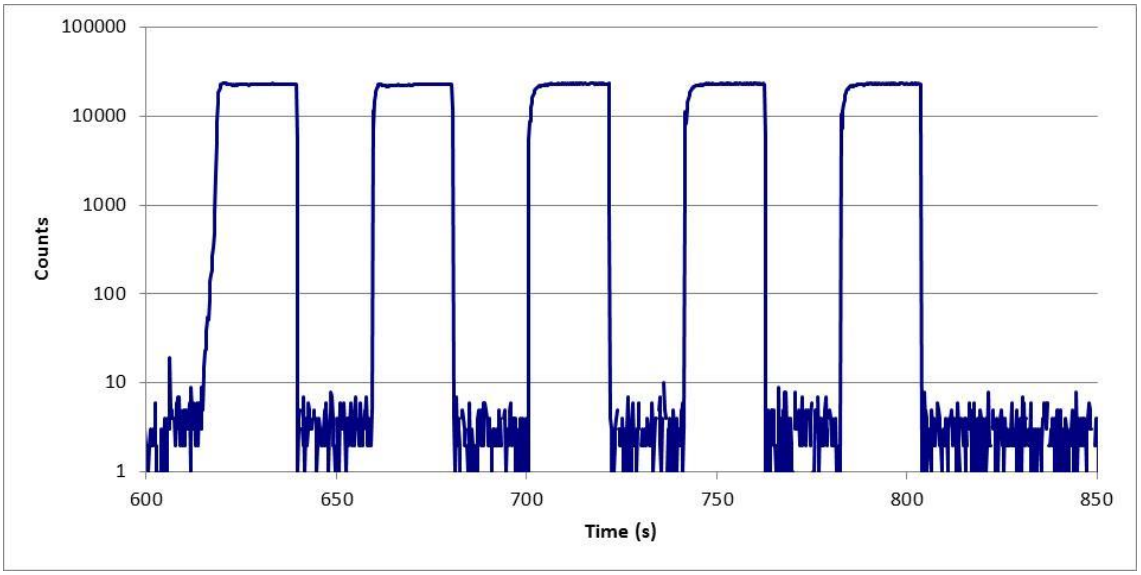

Figure 20. Plot of the count rate as a function of time for the DD/AWCC with the MP320 operating in slow pulse mode acquired using the LYNX digital signal processor module's MCS mode. In this example, neutrons were produced for 20 s, the generator shuts off, and delayed neutrons were counted for 20 s following each pulse. Note the clean start of each of the neutron irradiation cycles.

The rise and fall time of the neutron pulse using the Slow Pulse mode requires a delay of 0.2 s after the end of the neutron pulse before opening the delayed neutron counting window. With this constraint, we determine the optimal irradiation time, t_{irr}, and delayed neutron counting, t_{dn}, times per cycle to be 2.789 s and 1.116 s, respectively. A typical 30 min assay would consist of a 600 s background count followed by 278 irradiation cycles. With these parameters and assuming a source term of 2.5E6 n/s, the assay of a 200 g HEU item would provide an estimated measurement precision of 4.2%, in comparison the Am(Li)-based AWCC measurement would result in a measurement precision of 5.6%.

In theory, the Slow Pulse mode is a standard operating mode available on the MP320 and would provide the optimal measurement performance relative to the standard ^{252}Cf shuffler methodology. However, operation in the slow pulse mode results in the production of HV spikes in the neutron tube, potentially

damaging and reducing the life of the tube. Operation in this mode requires an override from the manufacturer that voids the tube warranty. Without this override, it is only possible to fire five pulses per hour in the slow pulse mode. Additionally, the Slow Pulse mode reduces the maximum operating voltage from 90 kV to 70 kV, reducing the maximum neutron yield by approximately a factor of 3. While in principle, it is possible to perform a 30 min assay using only five irradiation cycles (e.g., setting t_{irr} = 170, t_{dn} = 68 s), the resulting measurement precision would increase from 4.2% to 50%. Due to these limitations and the potential damage to the neutron generator, the slow pulse mode was investigated only in a cursory fashion.

5.3 DELAYED NEUTRON COUNTING: CYCLIC STEADY STATE MODE

5.3.1 Cycle Times for the Cyclic Steady State Mode

To provide the necessary neutron production on/off sequence for delayed neutron counting, a simple software code was developed to periodically turn the neutron generator on using its normal "soft start" sequence. This remote trigger method has two disadvantages relative to the Slow Pulse mode:

- **Timing:** The soft start up sequence requires a minimum of 7 s to begin neutron production. The soft shutdown requires approximately 12 s to complete and prevents restart of neutron production until the process is completed. This means a minimum of 19 s is required between irradiations. Of this 19 s interval, only the first 12 s period is available to delayed neutron counting.
- **Structure:** Approximately 7 s before initiation of neutron production there is a small pre-pulse of neutrons lasting approximately 2 s with a peak intensity of about 10% of the steady state intensity. To minimize the impact on the delayed neutron yield calculations, the interrogating neutron pulse must be long compared to the pre-pulse or at least 8 s in duration.

With these limitations we have defined the normal irradiation sequence to be 20 s neutron production on followed by 20 s off, counting delayed neutrons for a 5 s interval following irradiation. In terms of the traditional ^{252}Cf shuffler sequence, the following relevant timing applies:

- Irradiation time (t_{irr}): 20.0 s
- Delayed neutron count time (t_{dn}): 5.0 s
- Effective forward travel time (time after DN count to start of irradiation, t_f): 14.8 s
- Effective reverse travel time (time to neutron production has ceased, t_{rev}): 0.2 s
- Total time per cycle: 40.0 s

An example plot showing the count rate as a function of time for a type cyclic steady state measurement is shown in Figure 21. A 10 min background count is performed, followed by irradiation–delayed neutron counting cycles. An expanded view of the irradiation–delayed neutron counting cycles is provided in Figure 22. The small pre-pulse (note the log scale) is evident in the figure. Although the pre-pulse is not large, it precludes delayed neutron counting during the 7 s interval prior to the next pulse. We have found that the optimal delayed neutron count time per cycle, t_{dn}, is approximately 5 s. Because of the normal startup sequence for the MP320 the minimum time between pulses is fixed (approximately 19.6 s), we treat the 14.8 s between the end of delayed neutron counting and start of the next irradiation as the reverse travel time in the shuffler delayed neutron analysis. Essentially, this is wasted time during which the delayed neutron precusors decay away, and results in a degradation of measurement precision.

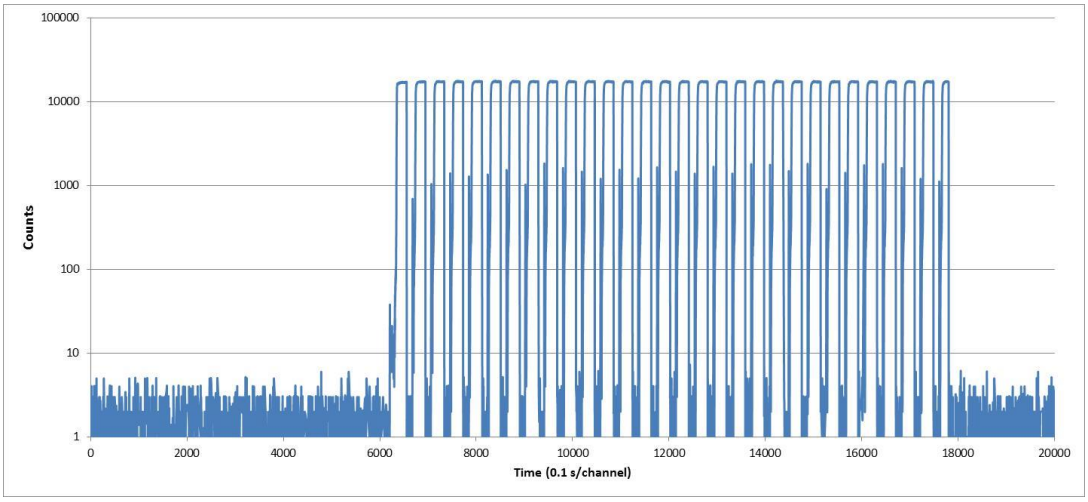

Figure 21. Plot of the count rate as a function of time for the DD/AWCC with the MP320 operating with periodic cycling of the generator showing the full count sequence of 30 cycles plus an initial 600 s background counting window (total assay time = 30 min).

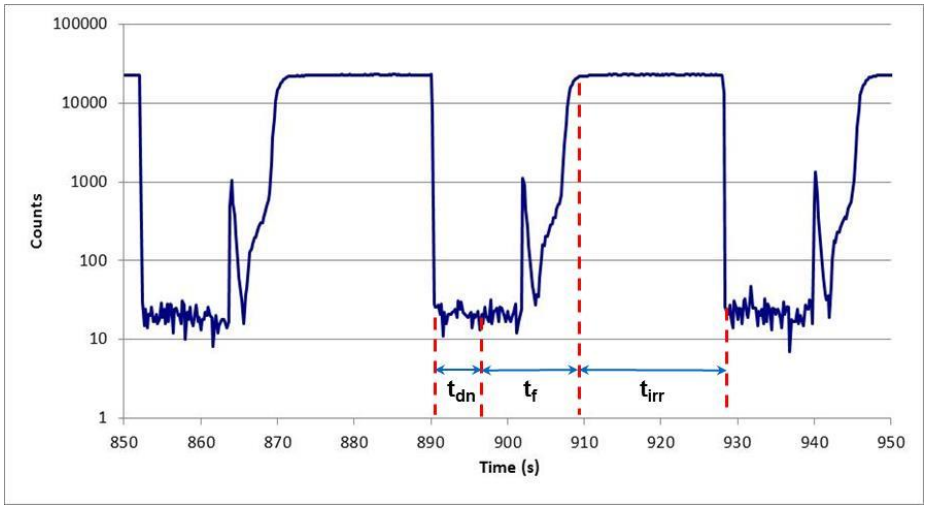

Figure 22. Plot of the count rate as a function of time for the DD/AWCC with the MP320 operating with periodic cycling of the generator. The small pre-pulse is a normal part of the MP320 firing sequence.

Analysis of the delayed neutron MCS spectrum is straight forward. The trailing edges of the neutron pulses are located using a standard edge search routine (e.g., a smoothed first derivative), the spectrum is sectioned using these edges (covering 28 s before through 12 s following the edge) and the sections aligned on the falling edge (Figure 23). The interrogating flux count rate is defined as the sum of counts in the 20 s before the edge divided by the total interrogation time (no. cycles × t_{irr}) and the delayed neutron count is the sum of counts in the 5 s following the edge divided by the total delayed neutron counting time (no. cycles × t_{dn}).

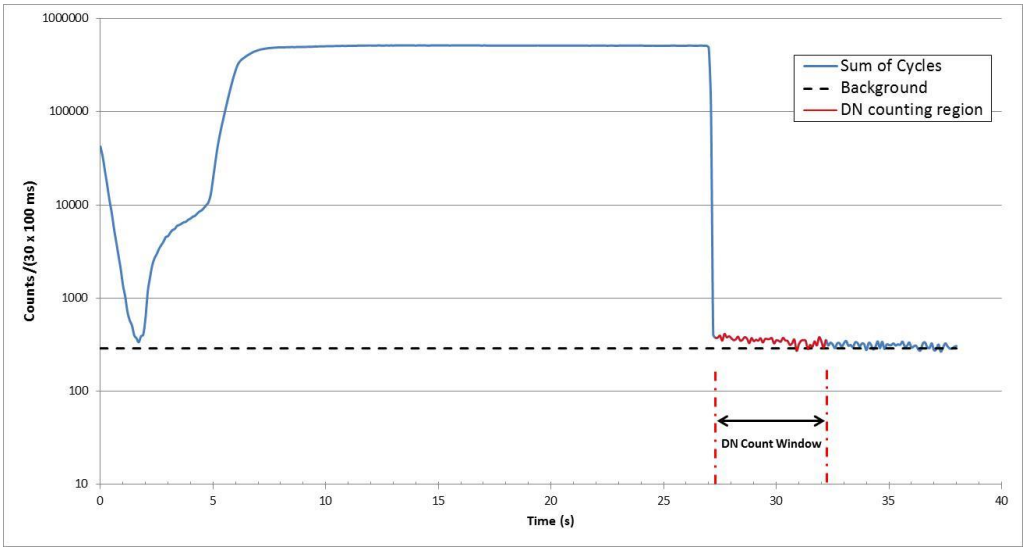

Figure 23. Plot of the summed cycle count rate as a function of time for the DD/AWCC. The cycles are aligned on the falling edge of the neutron pulse, and the summed cycles show a sharp cutoff. The decay of the delayed neutron population is evident in the delayed neutron counting window.

5.3.2 Delayed Neutron Counting: Cyclic Steady State Mode

To determine the potential performance of the delayed neutron measurement, the delayed neutron counting measurement was simulated using MCNPX (Pelowitz, 2008). The simulations provided estimates of the induced fission rate and neutron detection probability for a series of sample masses and enrichments. Since it is not possible to obtain meaningful measurement of the delayed neutron rates during the irradiation portion of the cycle, we can only count a fraction of the delayed neutrons produced per fission. The detectable delayed neutron fraction for the isotopes of uranium were estimated with standard buildup and decay algorithms using the eight delayed neutron group half-lives and intensities (Nichols, Aldama, & Verpelli, 2008) as illustrated in Figure 24 for the timing parameters listed above.

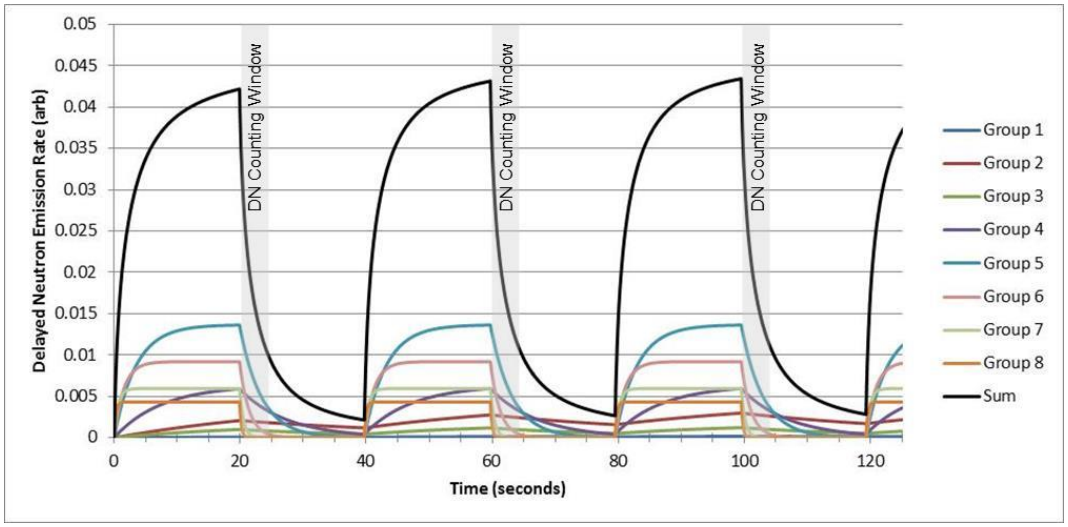

Figure 24. Buildup and decay of the 8 group delayed neutron populations within the modified LV-AWCC operated as a pseudo-shuffler. The shaded regions represent the delayed neutron counting windows (the interrogating neutron flux is not shown). A typical assay would include 21 interrogation cycles with alternating 20 s interrogation and 5 s delayed neutron counting window.

The simulated delayed neutron rates as a function of ^{235}U mass, for a series of containers of varying enrichment and mass of ^{235}U are presented in Figure 25. The enrichment dependence is somewhat more pronounced for the delayed neutron counting due to the higher delayed neutron yield per fission from ^{238}U compared to ^{235}U. The simulated count rates are replotted in Figure 26 as a function of the ^{235}U effective mass.

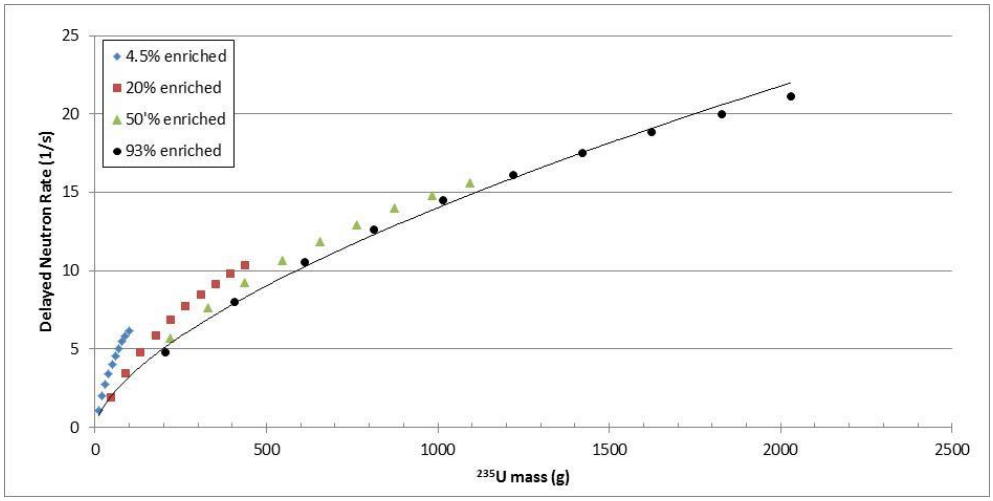

Figure 25. Simulated delayed neutron count rate as a function of ^{235}U mass for the modified LV-AWCC operated as a pseudo-shuffler (2.3E6 n/s interrogation rate, 20 s interrogation, 5 s delayed neutron counting).

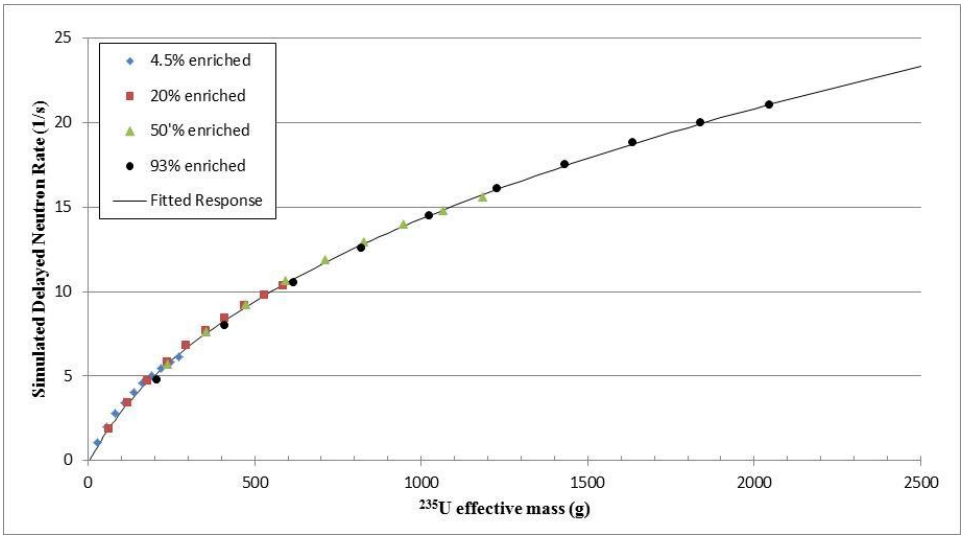

Figure 26. Simulated delayed neutron count rate as a function of ^{235}U effective mass for the modified LV-AWCC operated as a pseudo- shuffler (2.3E6 n/s interrogation rate, 20 s interrogation, 5 s delayed neutron counting [^{235}U effective mass = $m_{235} + 0.08\ m_{238}$]).

The conversion for ^{235}U effective mass is

$$m_{235\,effective} = m_{235} + 0.077 \cdot m_{238}$$

After correcting for the enrichment of the sample, the simulated rates follow a single response curve similar to that observed for the traditional AWCC measurement.

The expected count rate measurement precision for a total count time of 1800 s (time includes 600 s passive background count plus 30 cycles of 20 s irradiation and 5 s delayed neutron counting) is shown in Figure 27.

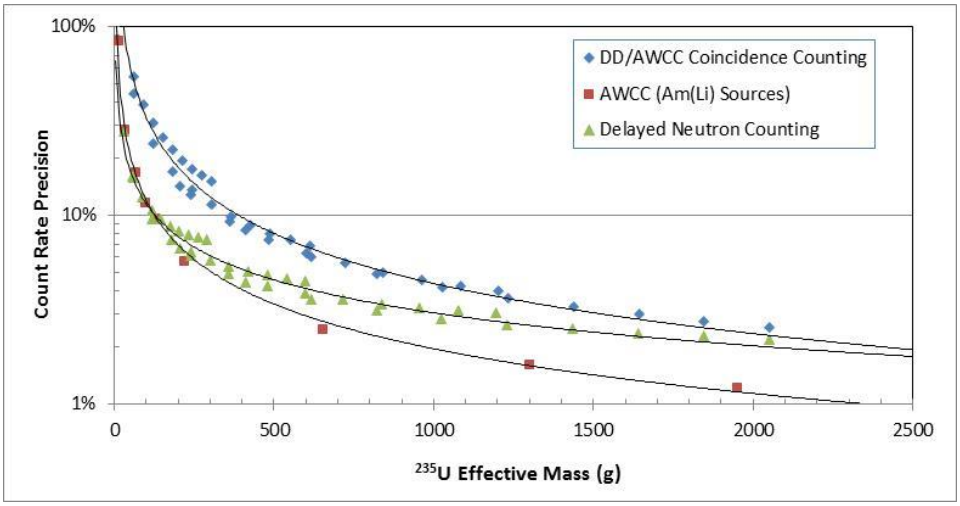

Figure 27. Expected measurement precision in the count rates as a function of $^{235}U_{effective}$ mass for the modified LV-AWCC operated in the AWCC and delayed neutron counting modes (1800 s assay time, 2E6 n/s D-D neutron interrogation rate). The performance for all three methodologies is based on a fast interrogation mode configuration. The scatter in the DD/AWCC data is related to the enrichment dependence of the measurement (i.e., the impact of the (alpha,n) emission and spontaneous fission rates on the background).

The observed measurement precision for the LV-AWCC operated in fast mode (all Cd liners installed) using Am(Li) neutron interrogation sources is presented for comparison. The expected precision in the assay mass result is determined by first fitting the simulated delayed neutron rates to a curve of the following form

$$R_{DN} = a \cdot \ln\left(m_{235\,effective}\right)^{b},$$

where *a* and *b* are empirically determined coefficients. The resulting curve is inverted and used to analyze the simulated rates as if they were actual measured values. The estimated error in the mass values are presented in Figure 28. The results indicate that for low mass values (<200 g ^{235}U effective) the delayed neutron measurement provides equivalent results to those of the traditional Am(Li)-based AWCC. However, as the mass increases above 200 g, the traditional AWCC outperforms the delayed neutron measurement.

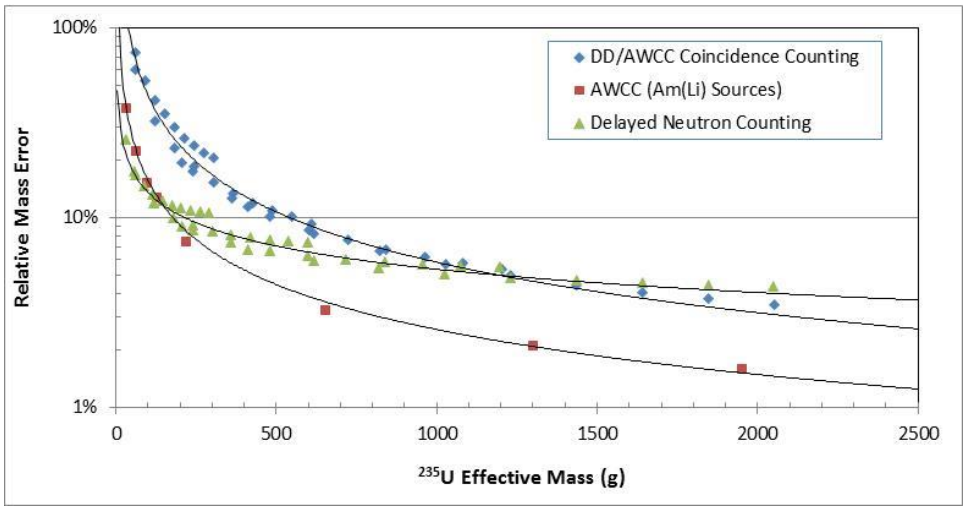

Figure 28. Expected measurement precision as a function of $^{235}U_{effective}$ mass for the modified LV-AWCC operated in the AWCC and delayed neutron counting (shuffler) modes (1800 s assay time, 2.2E6 n/s D-D neutron interrogation rate). The performance for all three methodologies is based on a fast interrogation mode configuration. The scatter in the DD/AWCC data is related to the enrichment dependence of the measurement and is not statistical in nature.

5.3.3 DD/AWCC Delayed Neutron Measurements

The DD/AWCC delayed neutron measurement cycle consisted of 10 min passive background followed by 30 cycles of 20 s irradiation, 5 s delayed neutron counting, and a 14.9 s delay until the generator restarts for the next cycle. Total measurement time for these assays is 30 min. Unlike the AWCC coincidence measurements, the delayed neutron measurements can be improved by increasing the interrogating neutron strength. For these measurements, the neutron generator was operated in continuous mode and cycled on/off (controlled by a simple 20 line code created in Python (Python Software Foundation. Python Language Reference, version 3.5. Available at http://www.python.org, 2017)) with the beam current and the HV bias set to 60 μA and 80 kV respectively providing an approximate neutron yield of 2.4E6 n/s during the 20 s irradiation time.

The uranium items listed in Table 2 were assayed (subject to availability) to demonstrate the performance of the delayed neutron measurement and provide validation of the MCNP modeling campaign. Table 6 provides the observed delayed neutron rates for each of the items weighted over all assays of that item. The single assay (total time 1800 s) measurement precision for each item is also provided in the table. A comparison of the MCNP predicted rates with the measured values is shown in Figure 29.

Table 6. Delayed neutron rates for the uranium test items

	U mass (g)	^{235}U effective mass (g)	Assays	Enrichment	Delayed neutron rate(cps)		Precision (1800 s)[a]
EMPTY	0.00	0.0	2	—	−0.14	± 0.19	—
NBS-071-078	169	14.6	3	0.2%	0.96	± 0.17	30%
U233-1	13.2	16.5	—	—	—	—	—
DU 5852	937	76.7	2	0.2%	1.26	± 0.24	27%
U233-2	63.0	78.8	2	—	1.53	± 0.72	66%
NBL001	195	51.5	1	20%	2.14	± 0.34	16%
NBL002	195	109.7	1	52%	3.12	± 0.34	11%
NBL003	195	182.4	9	93%	4.05	± 0.11	8%
YST-1-B	1,000	81.8	2	0.2%	2.72	± 0.25	13%
JAPO	8,000	654.7	2	0.2%	11.85	± 0.49	6%
JANY	18,000	1,473.1	3	0.2%	19.85	± 0.55	5%

[a] Uncertainties provided are the weighted average values for all of the assays of the item. The 1,800 s precision value represents the typical measurement precision for a 30 min count time.

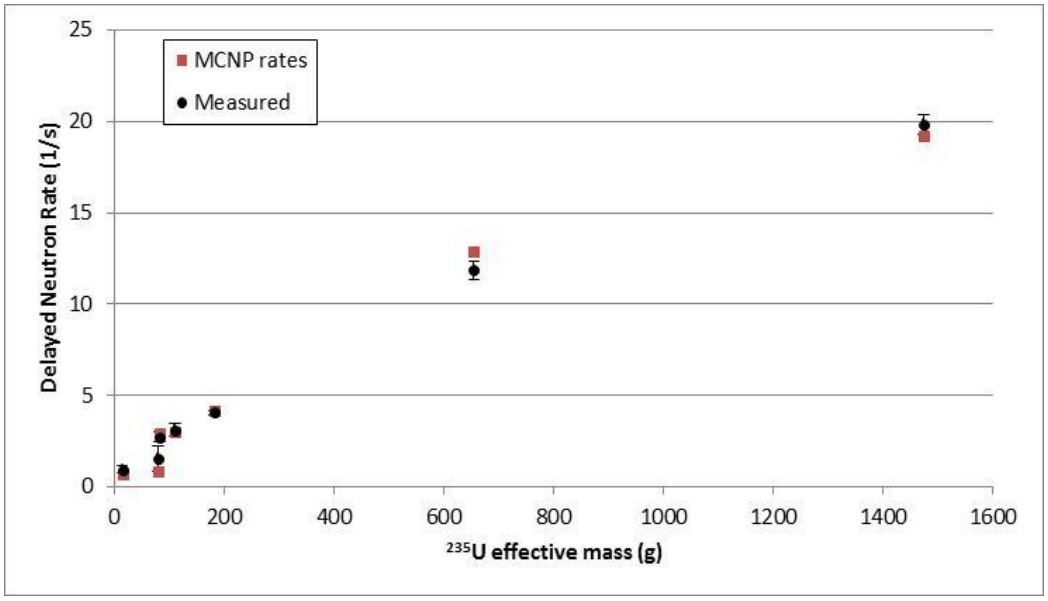

Figure 29. Comparison of the measured delayed neutron count rates for the DD/AWCC operated in the cyclic steady state mode with the MCNP simulated rates as a function of ^{235}U effective mass. The MCNP rate errors are not visible on the scale of this plot.

Figure 30 provides a comparison of the observed measurement precision for the LEU and HEU oxide items with the expected values from MCNP simulations. There is excellent agreement between the measured and expected values.

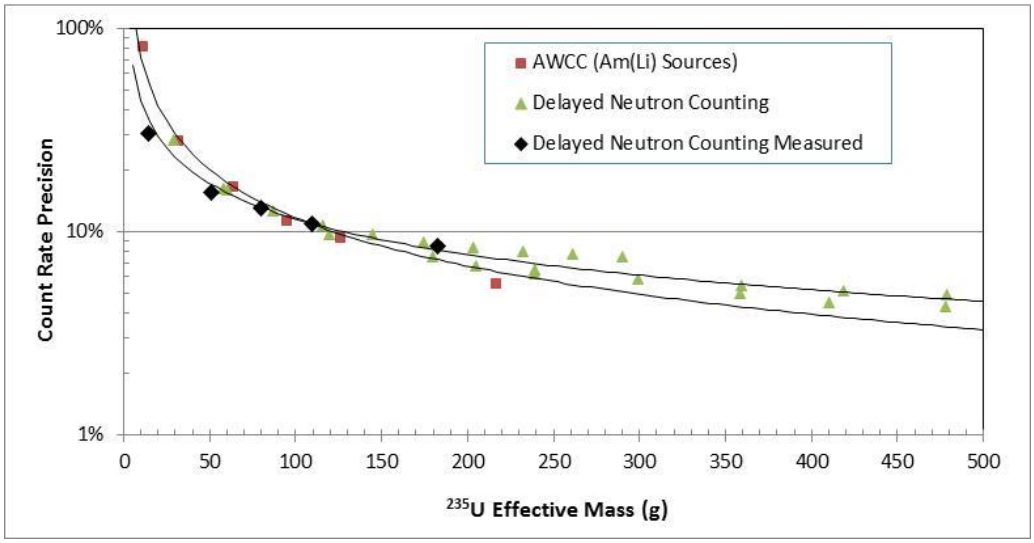

Figure 30. Comparison of the observed measurement precision in the delayed neutron count rates for the DD/AWCC operated in the cyclic steady state mode with the MCNP simulated rates as a function of ^{235}U effective mass for the uranium oxide items are shown.

The measurement precision of the delayed neutron assay is impacted by the passive neutron emission rate from the item. The passive neutron emission rates from the large metallic DU cylinders (JAPO and JANY) and the ^{233}U items are large in comparison to the empty chamber background rates and results in degradation of the measurement precision (Figure 31). However, although the measurement precision for DU items is approximately two times poorer than the LEU and HEU objects of the same ^{235}U effective mass, the delayed neutron count does not suffer the positive biases associated with the Am(Li)-based AWCC. For example the spontaneous fission rate from the DU item JANY provides the same coincidence doubles rate as 200 g HEU measured in the AWCC. Because the Am(Li)-based AWCC measurement has no background correction capability it would report a 200 g ^{235}U positive bias. The accuracy of the delayed neutron measurement is not so affected by the presence of the passive coincidence signal from the item because the delayed neutron assay incorporates a passive background measurement made possible by switching off the neutron generator.

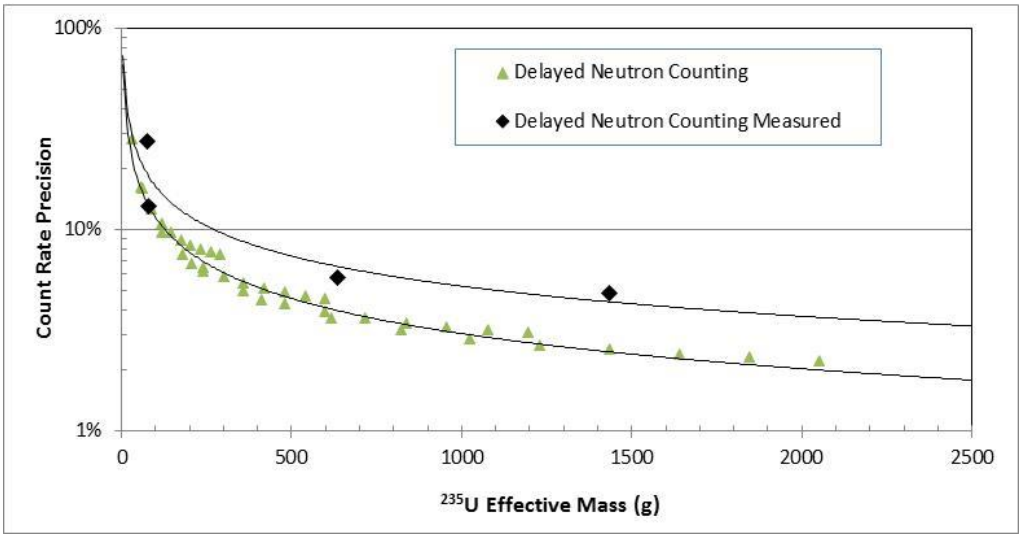

Figure 31. Comparison of the observed measurement precision in the delayed neutron count rates for the DD/AWCC operated in the cyclic steady state mode with the MCNP simulated rates as a function of ^{235}U effective mass for the depleted uranium items are shown.

5.4 DELAYED NEUTRON COUNTING: HIGH FREQUENCY PULSE MODE

An alternative approach to the traditional ^{252}Cf shuffler method for delayed neutron counting operates the neutron generator in its routine pulse mode at >100 Hz. A similar approach to delayed neutron counting was first suggested in 1984 by Caldwell et al. (Caldwell, Kunz, & Atencio, 1984) for the assay of transuranic waste using a D-T neutron generator with longer time scales; however, it is not clear that this method was ever implemented. This mode of operation avoids the lengthy start delays and pre-pulsing of the MP320 generator. This mode requires counting on microsecond time scales, which at first might seem to be a disadvantage; however, it emphasizes counting of delayed neutrons from the short-lived delayed neutron groups and can increase the fraction of delayed neutrons available for counting by a factor of 2 or more. In comparison to the cyclic mode described above, the available delayed neutron fraction increases from 0.125 to 0.5, or a factor of 4 improvement for ^{235}U.

5.4.1 Cycle Times for the High Frequency Pulse Mode

The minimum pulse frequency available on the MP320 generator is 250 Hz, so the total time per cycle is 4 ms. Examination of the MCNP simulated time response of the DD/AWCC and the measured time history for the DD/AWCC shows it takes a minimum time of 1 ms for the interrogating neutrons to completely die away in the counter. Using the constraints of 4 ms total cycle time, 1 ms "reverse travel" time, 0 ms forward travel time, and $t_{irr} + t_{dn} = 3$ ms, the best measurement precision is achieved when $t_{irr} = 2$ ms and $t_{dn} = 1$ ms. However, for these test measurements we selected a less optimal time sequence that would allow us to verify that the net counts in the delayed neutron counting window are, in fact, due to delayed neutrons. To accomplish this verification, we selected an irradiation time of 1 ms and compared the net count rates in three overlapping delayed neutron counting time windows. If the net count rates are the same for each of the time windows, then we can conclude that we are counting delayed neutrons and not a long thermalization tail from the irradiation (i.e., that 1 ms is sufficiently long to wait before opening the delayed neutron counting window).

Configuration	1	2	3
Irradiation time (t_{irr})	1.0	1.0	1.0 ms
Delayed neutron count time (t_{dn})	1.0	1.5	2.0 ms
Effective forward travel time(t_f)	0.0	0.0	0.0 ms
Effective reverse travel time(t_r)	2.0	1.5	1.0 ms
Total time per cycle	4.0	4.0	4.0 ms

To enable counting for the fast pulse mode, a timing signal available from the MP320 was used to synchronize the MCS sweep with the neutron pulses (Figure 32).

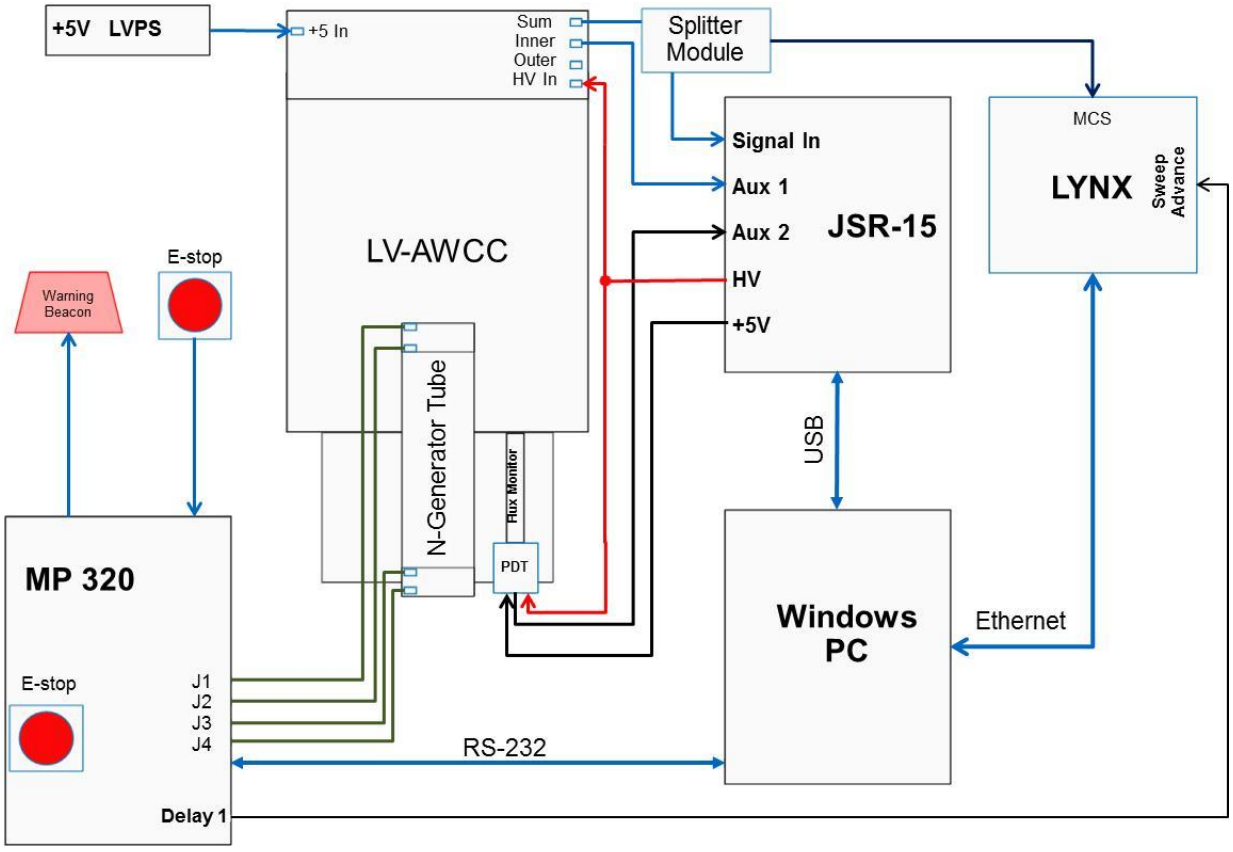

Figure 32. Diagram showing the electronics configuration for the DD-AWCC configured for the fast pulse mode delayed neutron counting.

If passive coincidence counting is not required, the JSR-15 shift register could be replaced by a second multi-channel scaling module (e.g., a LYNX) as shown in Figure 33. This arrangement would minimize the types of electronics modules contained in the system.

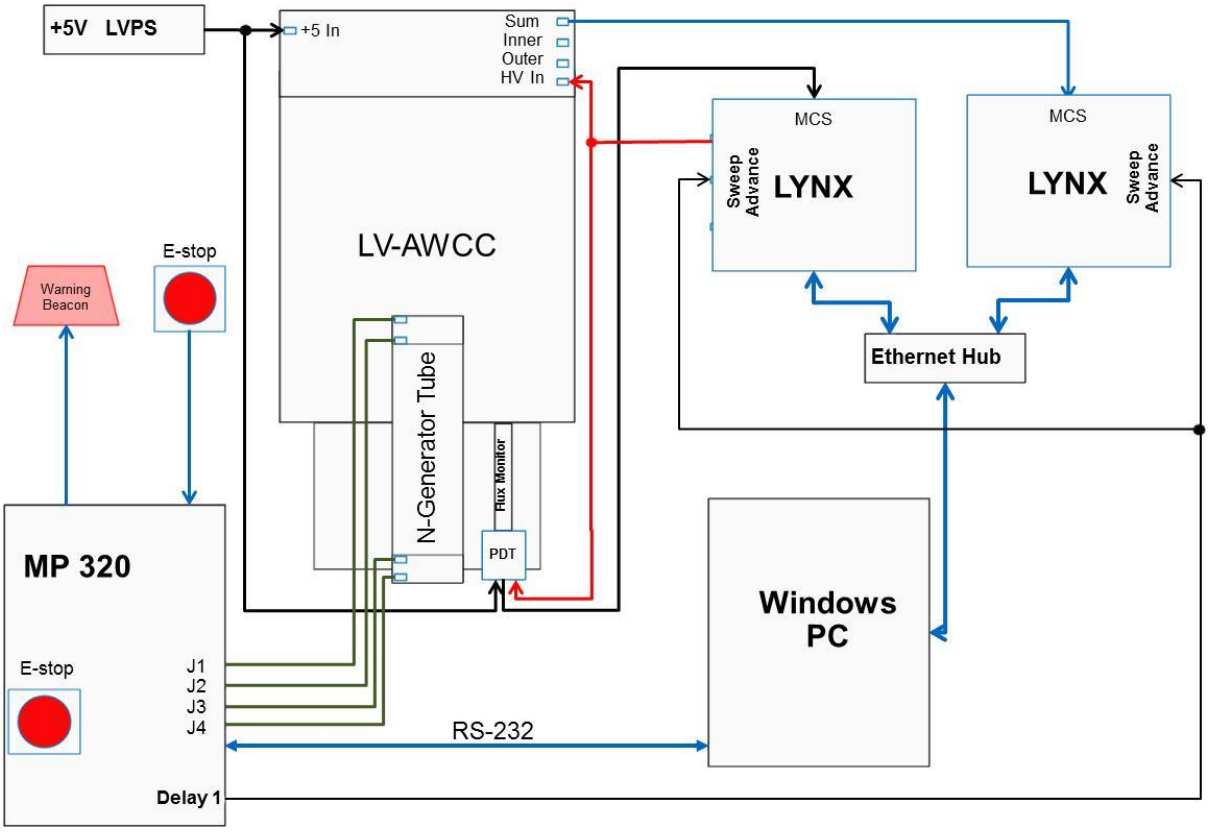

Figure 33. Diagram showing an alternative electronics configuration for the DD-AWCC for the fast pulse mode delayed neutron counting. The JSR-15 is replaced by a second multi-channel scaling module.

5.4.2 High Frequency Pulse Mode Delayed Neutron Counting

For easier comparison purposes with coincidence and traditional delayed neutron measurements we have configured the high frequency pulse mode for 30 min total measurement time. The measurenment will consist of 10 min passive background count, followed by 20 min of active interrogation.

Operation of the neutron generator at 250 Hz for a 20 min active interrogation results in 300,000 individual interrogation cycles. Because of the low number of counts each cycle (Figure 34) and the large number of interrogating cycles, the MCS sweep is reset at the beginning of each neutron pulse from the generator such that the 300,000 time histories for each cycle are summed during the meaurement. The resulting trace for a typical measurement is shown in Figure 35.

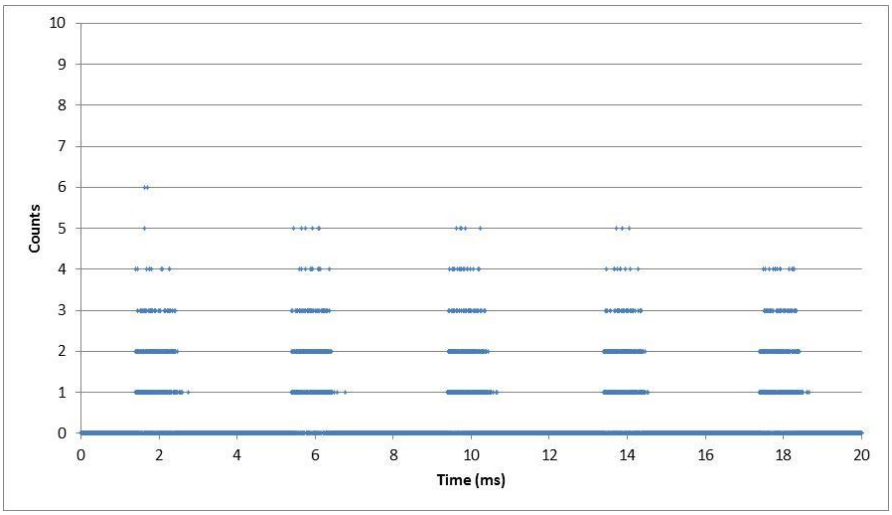

Figure 34. Plot of the count rate as a function of time for the DD/AWCC with the MP320 operating with a 250 Hz repetition rate (multi-channel scaling conversion = 10 µs/channel.

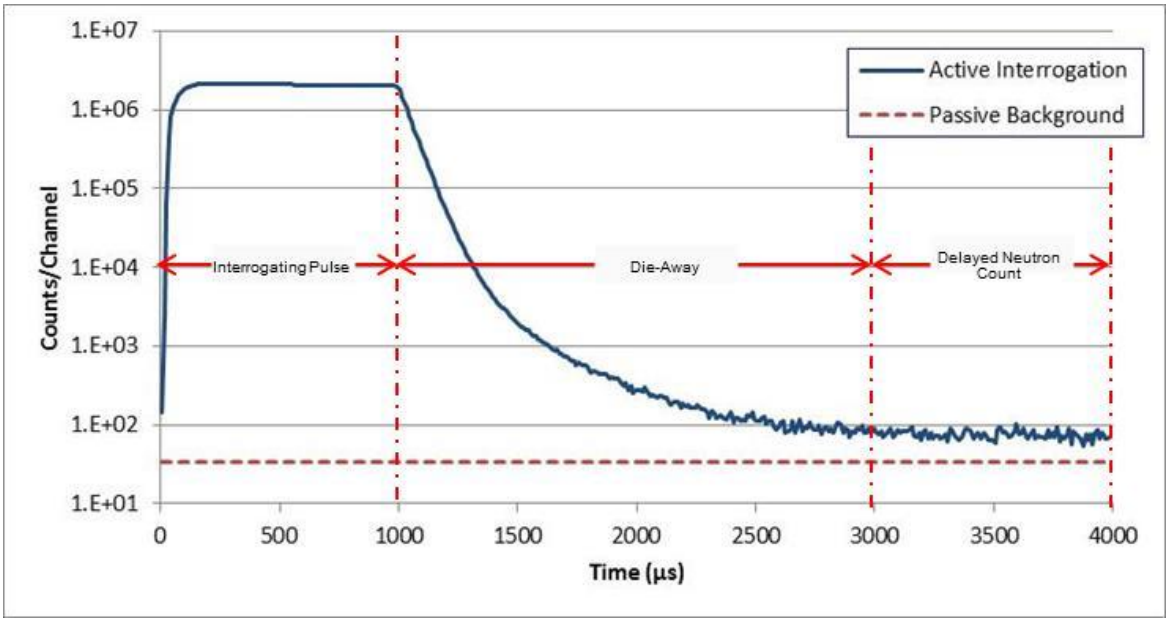

Figure 35. Plot of the count rate as a function of time for the DD/AWCC with the MP320 operating at a 250 Hz repetition rate with the MCS sweep synched to the generator pulse. The plot represents the sum of 300,000 generator pulses and 2 µs/channel.

Neutron Generator Yield

Operation of the neutron generator in its normal pulsing mode provides a higher interrogating neutron yield for the shuffler measurement than the steady state mode. One of the characteristics of pulsed neutron generators is that the maximum yield is a time-averaged value. Operating the generator with a 25% duty cycle (1 ms on, 3 ms off) results in approximately a factor of 4 increase in the interrogating neutron rate compared with the steady state mode. The effective yield for the generator settings beam current = 60 µA, high voltage = 60 kV, 250 Hz, with 25% duty factor was 1.05E7 n/s.

The count rate during each cycle is divided into the interrogation, die-away, and delayed neutron counting windows. The interrogating window includes the period during which the neutron generator is producing neutrons in this case the interrogation lasts 1 ms. The die-away window includes the period when the neutron generator pulse is completed but neutrons within the HDPE shield are slowing down prior to detection. (Note: Unlike the differential die-away systems, this neutron population exists primarily outside the assay cavity and does not continue to induce fission events within the sample and does not impact the delayed neutron emission rate.) Examination of the die-away behaviour is accomplished by a comparison of the net neutron count rate (passive neutron background subtracted) as a fuction of time for a uranium item and the empty assay cavity. Figure 36 shows the net active count rate as a function of time for the 8 kg DU cylinder, JAPO, and the emtpy chamber, and Figure 37 shows the difference between these two spectra. The net count rate becomes constant with time starting no more than 200 µs following termination of the neutron pulse. Had the die-away component included induced fission events, we would expect to see the net count rate in Figure 37 decrease with time.

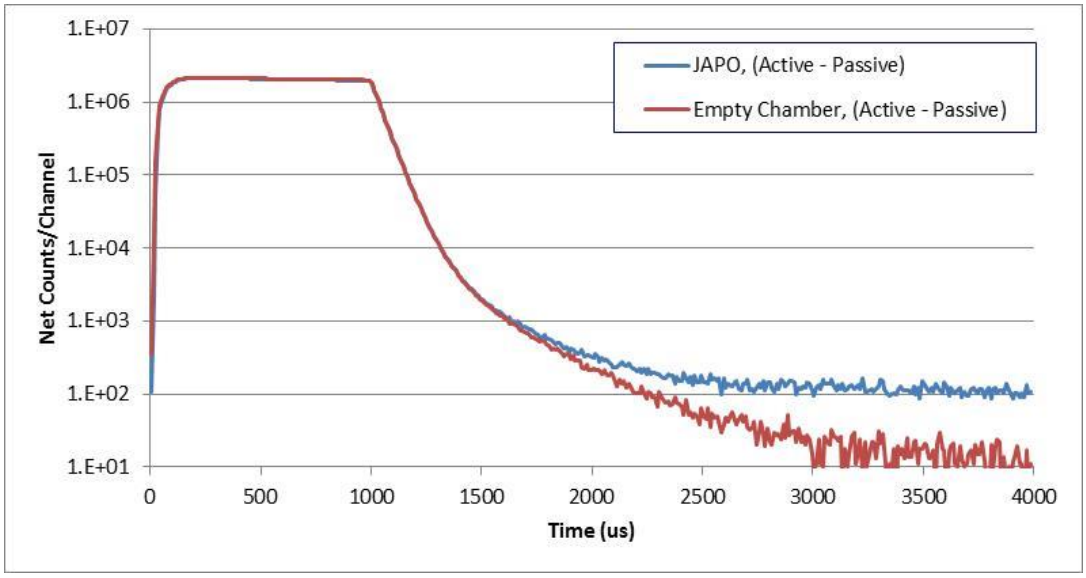

Figure 36. Comparison of the passive background corrected count rates as a function of time for the DD/AWCC with the MP320 operating at a 250 Hz repetition rate for the 8 kg DU cylinder, JAPO, and the empty assay cavity.

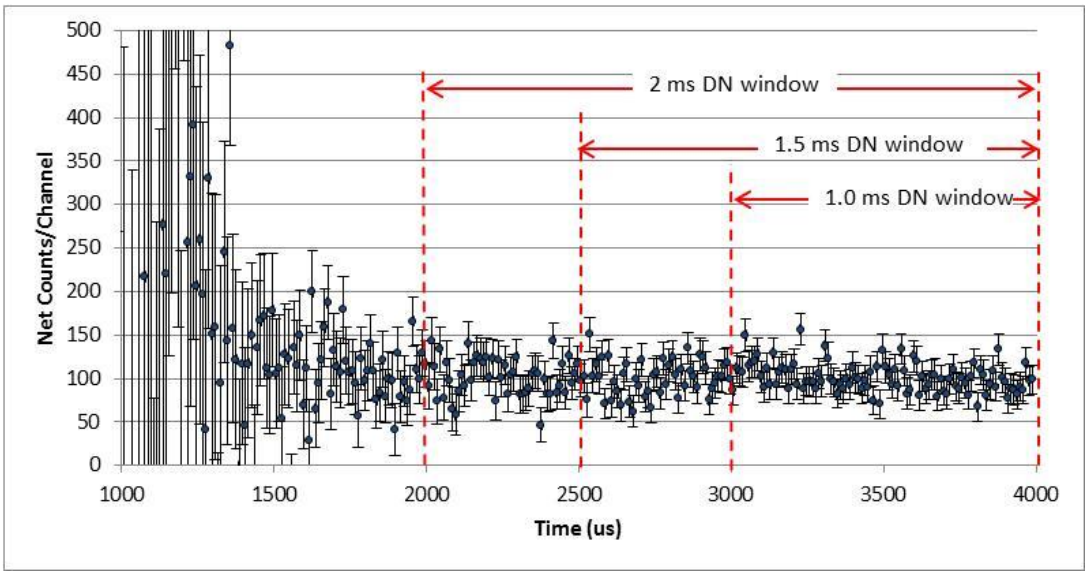

Figure 37. Plot of the net active counts for the 8 kg DU cylinder. The lack of an apparent slope to the net signal confirms the net active signal is a result of delayed neutron emission. Delayed neutron count rates determined using each of the three windows are statistically equivalent.

5.4.3 High Frequency Pulse Mode Delayed Neutron MCNP Simulations

The simulated delayed neutron rates as a function of ^{235}U mass, for the series of containers used in the above evaluations were reevaluated using the revised timing sequence for the high frequency interrogation. Since the enrichment dependence seen in the coincidence counting and traditional shuffler modes is primarily due to the induced fission process, we expect to see the same enrichment dependences for the high frequency interrogation mode. The delayed neutron rates for the high frequency interrogation mode as a function of enrichment and ^{235}U mass are presented in Figure 38.

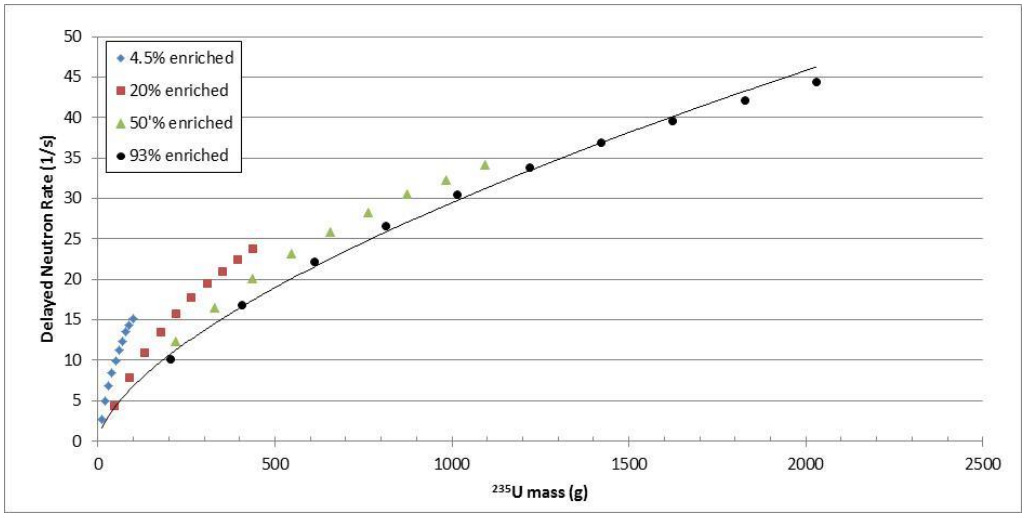

Figure 38. Simulated delayed neutron count rate as a function of ^{235}U mass for the modified DD/AWCC operated with the neutron generator operating in the high frequency mode (250 Hz, 1.05E7 n/s interrogation rate, 20 s interrogation, 5 s delayed neutron counting).

The enrichment dependence is similar to that of delayed neutron counting results shown in Figure 25. The conversion for ^{235}U effective mass determined by a fit to the MCNP simulation results is

$$m_{235\,effective} = m_{235} + 0.083 \cdot m_{238}$$

After correcting for the enrichment of the sample, the simulated rates follow a single response curve as shown in Figure 39.

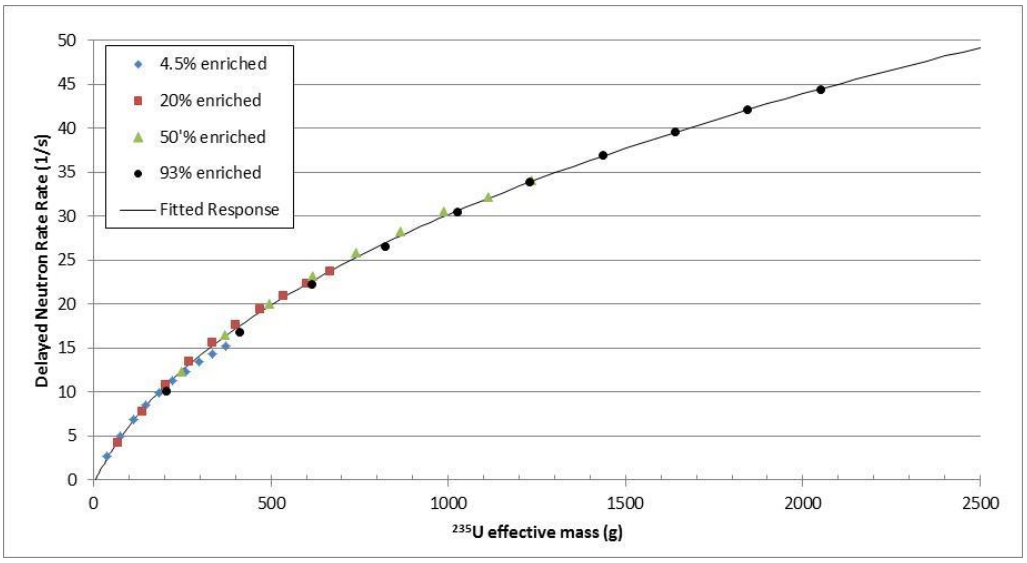

Figure 39. Simulated delayed neutron count rate as a function of ^{235}U effective mass for the modified DD/AWCC operated in the high frequency mode.

The expected measurement precision in the delayed count rates for a total count time of 1800 s (time includes 600 s passive background count plus 300,000 cycles of 1 ms irradiation and 2 ms delayed neutron counting) is shown in Figure 40.

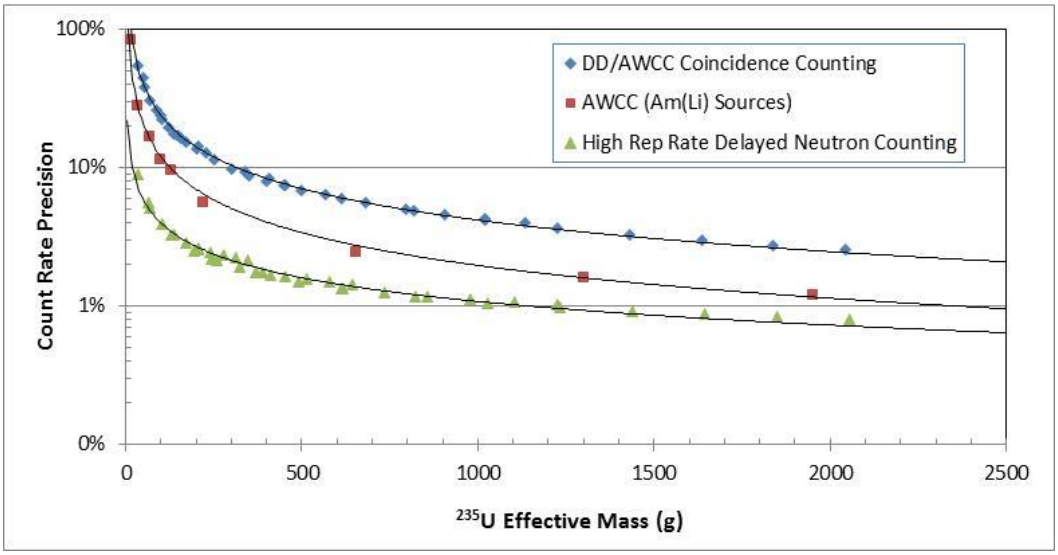

Figure 40. Expected measurement precision in the count rates as a function of $^{235}U_{effective}$ mass for the modified LV-AWCC operated in the AWCC and delayed neutron counting modes (1800 s assay time, 250 Hz interrogation rate). The performance for all three methodologies is based on a fast interrogation mode configuration.

The observed measurement precision for the DD/AWCC operated in fast mode (all Cd liners installed) using Am(Li) neutron interrogation sources is presented for comparison. The expected measurement precision using the delayed neutron counting approach operated in the high rate pulse mode betters that obtained from the traditional AWCC method by a factor of 2 to 3 for the same total assay time. Finally, the expected precision in the assay mass result is determined by first fitting the simulated delayed neutron rates to a curve of the following form

$$R_{DN} = a \cdot \ln\left(m_{235\,effective}\right)^{b},$$

where *a* and *b* are empirically determined coefficients. The resulting curve is inverted and used to analyze the simulated rates as if they were actual measured values. The estimated errors in the assay mass values are presented in Figure 41. The results indicate that for mass values less than 500 g ^{235}U effective, the high frequency delayed neutron measurement provides a factor of 2 better measurement performance compared to the traditional Am(Li)-based AWCC. However, as the mass increases above 500 g, the difference in measurement precision narrows.

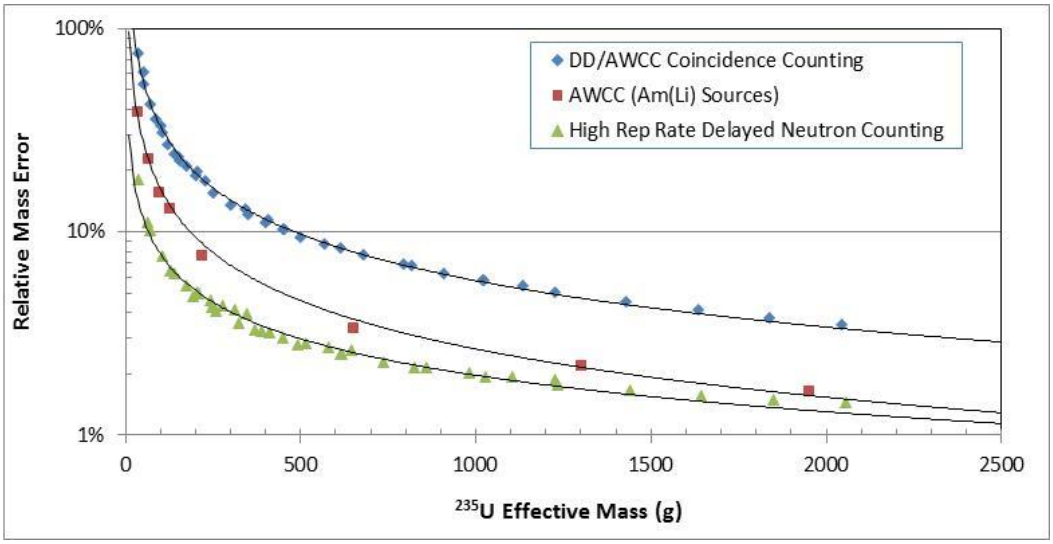

Figure 41. Expected measurement precision as a function of $^{235}U_{effective}$ mass for the modified LV-AWCC operated in the AWCC and DN counting modes (1800 s assay time, 250 Hz interrogation rate). Note that the performance for all three methodologies is based on a fast interrogation mode configuration.

5.4.4 High Frequency Pulse Mode Delayed Neutron Measurements

The uranium items listed in Table 2 as well as some additional items were assayed to confirm the MCNP predicted performance and to provide direct measurement performance results for the DD/AWCC operated in the high frequency mode. The neutron generator was set to operate at 250 Hz, with beam current of 60 µA and high voltage of 80 kV. For each item assayed, the delayed neutron count rate was evaluated for three different time windows to confirm that the observed counts are due to delayed neutron events and not additional induced fission. The 250 Hz operation of the neutron generator sets the total cycle time at 4 ms. In each case the irradiation time is 1 ms, while the effective reverse travel time (during which the thermal neutron flux in the shielding decays away) is set to 1, 1.5, or 2 ms, leaving 2, 1.5 or 1 ms for the delayed neutron counting window. The following counting configurations were used for the measurements:

Configuration	1	2	3
Irradiation time (t_{irr})	1.0	1.0	1.0 ms
Delayed neutron count time (t_{dn})	1.0	1.5	2.0 ms
Effective forward travel time(t_f)	0.0	0.0	0.0 ms
Effective reverse travel time(t_r)	2.0	1.5	1.0 ms
Total time per cycle	4.0	4.0	4.0 ms

The measured delayed neutron count rates are presented in Table 7. For each item assayed, the observed count rate is independent of the time window. To validate the MCNP modeling results, a comparison of the measured rates with the MCNP simulated rates for the DU, LEU, and HEU items assayed is presented in Figure 42 and Figure 43. The simulated and measured rates agreed to within 2 sigma for each item. A comparison of the expected measurement precision from the MCNP modeling with observed measurement precision is presented in Figure 44, showing excellent agreement.

Table 7. Delayed neutron count rates for the high frequency pulse mode measurements

Item	Total SNM (g)	^{235}U Enrich.	^{235}U Effective mass (g)	Assays	Delayed neutron count rates (cps)					
					t_{open} = 1.0 ms, t_{dn} = 2.0 ms		t_{open} = 1.5 ms, t_{dn} = 1.5 ms		t_{open} = 2.0 ms t_{dn} = 1.0 ms	
JAP0	8,000	0.2%	630.8	1	33.93	± 0.50	34.11	± 0.54	34.02	± 0.62
JANY	18,000	0.2%	1,419.2	3	54.86	± 0.39	54.77	± 0.42	54.48	± 0.49
DU5852	937	0.2%	73.9	1	9.28	± 0.27	9.72	± 0.29	9.86	± 0.33
YST-1-B	1,000	0.2%	78.8	2	6.54	± 0.20	6.55	± 0.21	6.53	± 0.24
NBS071-078	169	0.71%	14.1	4	1.13	± 0.13	1.43	± 0.13	1.41	± 0.14
NBL003	**195**	**93.2%**	**182.7**	**8**	**8.23**	**± 0.10**	**8.49**	**± 0.11**	**8.58**	**± 0.12**
NBL002	195	52.5%	109.4	5	6.24	± 0.12	6.34	± 0.13	6.43	± 0.14
NBL001	195	20.1%	51.2	4	3.71	± 0.13	3.81	± 0.14	3.96	± 0.15
U233-2	14	—	—	3	1.36	± 0.22	1.26	± 0.23	1.47	± 0.26
U233-3	13.2	—	—	4	0.88	± 0.16	0.92	± 0.17	0.82	± 0.19
U233-5	32	—	—	12	2.25	± 0.15	2.13	± 0.16	1.99	± 0.18
U233-6	91	—	—	20	7.56	± 0.23	7.43	± 0.25	7.67	± 0.28
Empty	0	—	0.0	6	−0.04	± 0.10	−0.02	± 0.10	−0.01	± 0.11
NBL Blank	0	—	0.0	2	−0.47	± 0.17	−0.41	± 0.17	−0.29	± 0.19
Pu oxide	30	WG	—	2	7.76	± 1.09	8.77	± 1.18	7.57	± 1.34

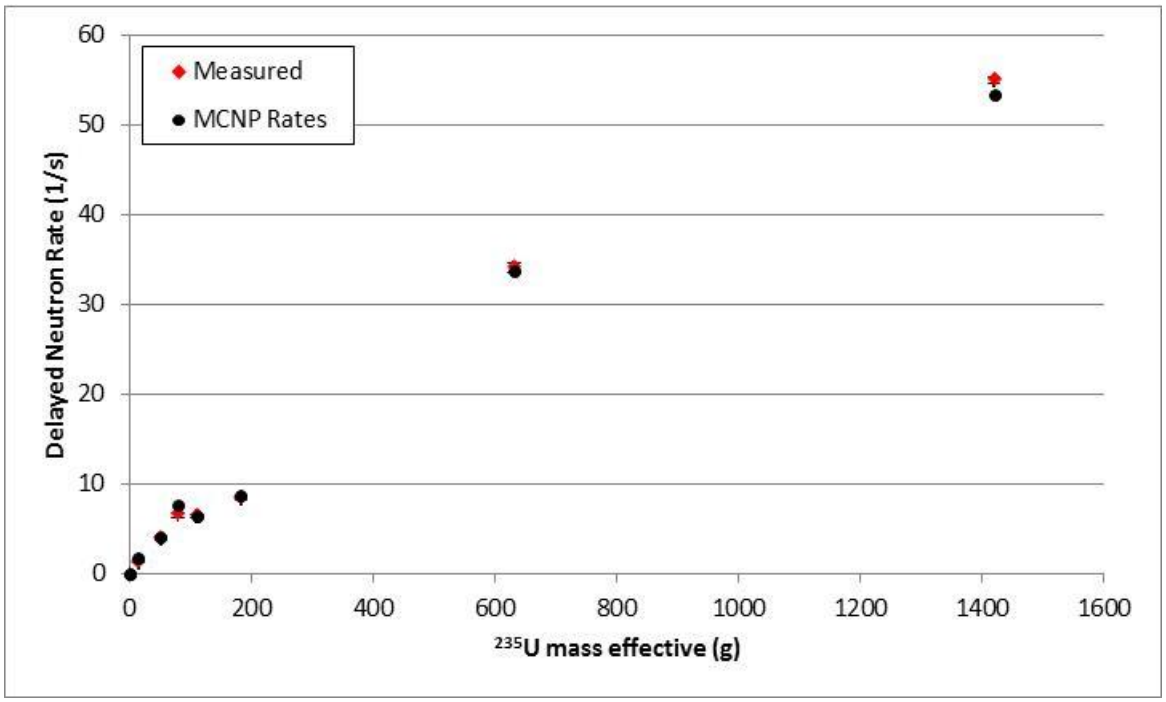

Figure 42. Comparison of the MCNP simulated delayed neutron rates with the measured values for the DU, LEU, and HEU items shown in Table 7 with the DD/AWCC operated in the high frequency mode.

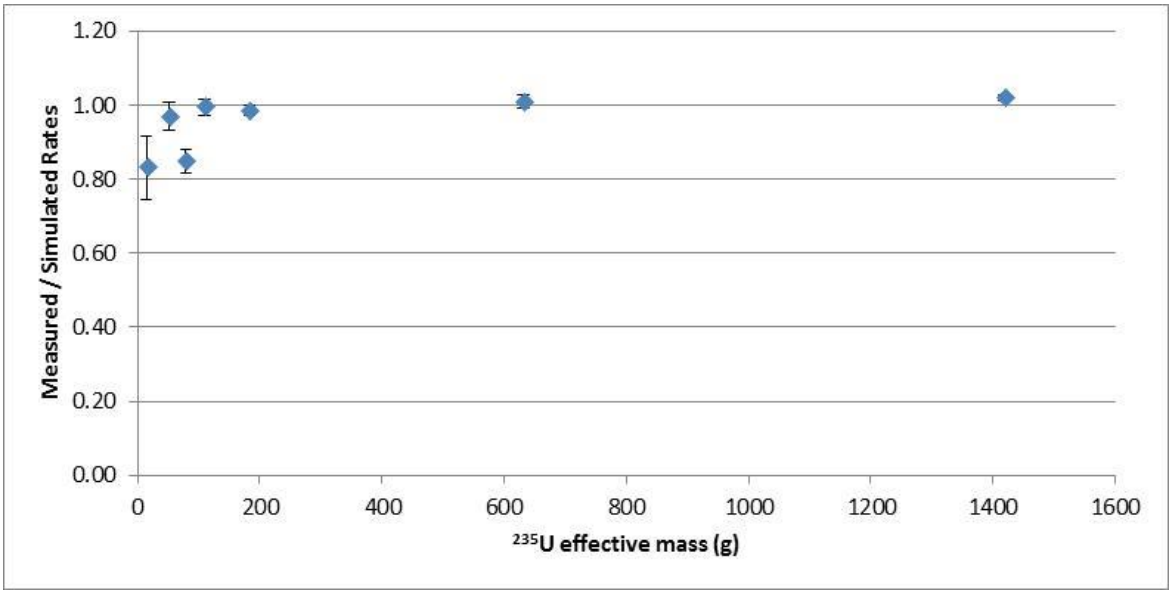

Figure 43. Comparison of the ratio of the measured values to the MCNP simulated delayed neutron rates with for the DU, LEU, and HEU items shown Table 7 with the DD/AWCC operated in the high frequency mode.

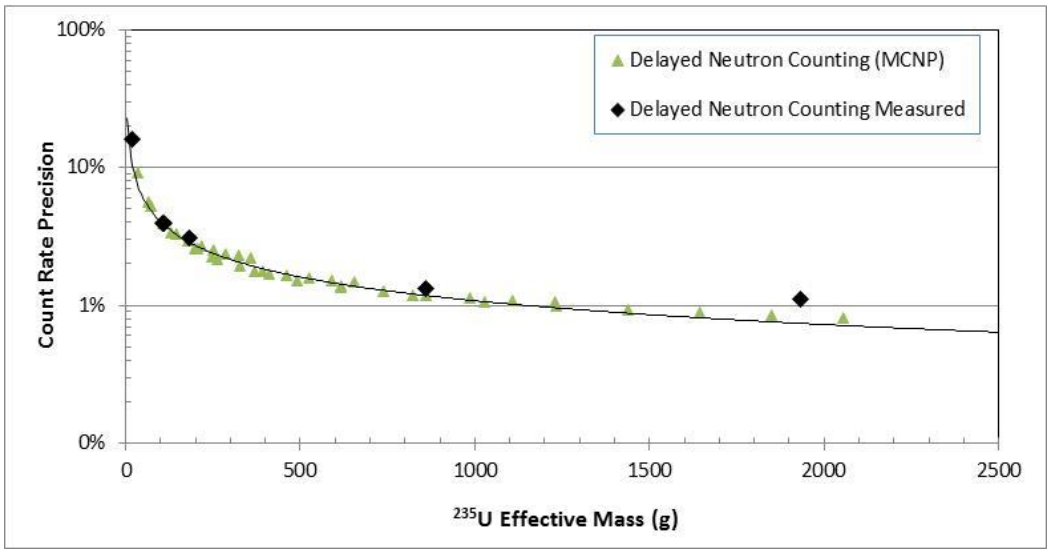

Figure 44. Comparison of the MCNP simulated delayed neutron rate precision with the observed values with the DD/AWCC operated in the high frequency mode.

6. CONCLUSION

The relatively large size of the MP320 neutron tube adversely impacted the performance of the DD/AWCC system. The 12.5 cm diameter of the tube, and the position of the neutron production target line 12.5 cm from the end of the tube, reduced the amount of shielding possible between the ^{3}He tubes and the interrogating neutron source, which resulted in reduced interrogating neutron flux on the sample. The resulting system provides equivalent linearity but requires five times longer to achieve the same measurement precision as the traditional Am(Li)-based measurement. However, this study demonstrates the physics feasibility of the DD/AWCC approach, and with a different generator configuration performance will improve. Adopting the delayed neutron counting methodology of the ^{252}Cf shuffler offers improved measurement precision (a factor of 2 or greater) over the traditional AWCC measurement without loss of accuracy.

The MCNP simulations and direct measurements performed to date demonstrate that the D-D neutron generator is a viable alternative to the isotopic Am(Li) neutron sources used in the current generation of AWCC.

The original concept for this project was to integrate a new generation compact D-D neutron generator into the LV-AWCC, such as Berkeley Lab's Mini Neutron Tube (~8 mm OD × 20 mm with 1E7 n/s yield) (Leung). However, we found that, in general, compact neutron generators were either not so compact, provided low neutron yields, or could not be considered COTS items. However, we expect such generators to be commercially available in the near future. With a more compact neutron generator, source-sample coupling can be improved, and the emitted neutrons can be better shielded from direct detection by the AWCC, resulting in improved performance as a traditional AWCC. The more compact generators will also eliminate the need to mount the AWCC on a pedestal and will simplify the retrofit of existing AWCC systems with D-D generators. Integration of a more compact neutron generator will also enhance the delayed neutron counting regime of the DD/AWCC through improvement of the source-sample coupling and increased induced fission rates.

Active Well Coincidence Counting (AWCC) Limitations

- Measurement precision of the DD/AWCC in active coincidence counting is limited by the geometric form factor of the MP320 generator. The distance between the end of the neutron tube and the neutron production target line, 13 cm, and results in poor source-sample coupling and the diameter of the generator tube reduces the amount of HDPE shielding between the neutron production and the ^{3}He detector tubes Essentially, not enough of the source neutrons reach the sample.

    - A more compact generator tube that reduces the target line distance to less than 5 cm and the tube diameter from 13 to ~6.5 cm will provide sufficient improvement so the performance of the generator-based system could equal or exceed that obtained with the Am(Li) sources.

- Use of a single generator in place of the two Am(Li) interrogation sources results in a significant reduction in sensitivity as a function of height within the assay cavity. For relatively uniform containers of pellets or powers, this dependence is rolled up into the mass calibration curve. However, additional spatial uncertainties can be expected for heterogeneous items.

Delayed Neutron Counting: Slow Interrogation Rate

- Measurement precision of the DD/AWCC in active coincidence counting is limited by the geometric form factor of the MP320 generator. The long distance between the end of the neutron tube and the neutron production target line, again results in poor source-sample coupling. However, in this case the large diameter of the tube is not a limiting factor.

    - A more compact generator tubee that reduces the target line distance to less than 5 cm is required.

    - Alternatively, a somewhat higher yield neutron generator is required. The MP320 maximum in steady state mode is approximately 2E6 n/s. To equal the performance of the current AWCC with two Am(Li) sources, a generator of the same form factor as the MP320 requires a yield of 1E7 n/s.

- The delayed neutron counting measurement precision is highly dependent on room background. Neutron source movement in the vicinity of these measurements must be restricted or additional shielding will be required about the AWCC.

- Operation of the MP320 in Slow Pulse mode—had this function been truly available—would allow delayed neutron counting timing similar to that used in the ^{252}Cf shufflers (e.g., 7 s irradiation followed by 7 s delayed neutron counting).

    - This would increase the fraction of delayed neutrons available for counting and lead to improved measurement precision with performance equivalent to that provided by the Am(Li)-based measurement.

    - This mode would also allow simultaneous acquisition of active coincidence counting and delayed neutron counting in the same assay cavity.

    Having extended capability for the Slow Pulse mode (i.e. not limited to 5 bursts per hour) would be a desirable feature in future neutron generators.

Delayed Neutron Counting: Fast Interrogation Rate

This non-traditional delayed-neutron analysis method takes advantage of the compression of the generated neutrons into a smaller time interval to provide a significantly higher interrogating source strength than is available in the steady state operating mode without increasing personnel exposure rates.

The increase in interrogation strength combined with a higher fraction of delayed neutrons available for detection provides a factor of 10 improvement in signal strength compared to operation with the time sequences typical of the ^{252}Cf shuffler. The resulting measurement provides a factor of 2 improvement in measurement precision for the same total assay time compared to the Am(Li)-based AWCC measurement. Further improvements to the measurement precision may be possible through additional optimization of the measurement geometry, for example:

- The use of a borated poly shield about the generator housing.
- Availability of a more compact neutron generator
- Availability of a lower repetition rate (e.g. 100 Hz) neutron generator.

7. REFERENCES

[1] H. O. Menlove. 1979. "Description and Operation Manual for the Active Well Coincidence Counter." Rep. No. LA-7823-M. Los Alamos National Laboratory, Los Alamos, NM.

[2] D. B. Pelowitz. 2008. "MCNPX User's Manual." Version 2.6.0. Rep. No. LA-CP-07-1473, Los Alamos National Laboratory, Los Alamos, NM.

[3] R. D. McElroy Jr., S. L. Cleveland, S. Croft, and A. L. Lousteau. 2016. "The D-D Neutron Generator as an Alternative to Isotopic Neutron Sources in International Safeguards." in *Proceedings of the 57th Annual Meeting of the Institute of Nuclear Materials Management*, Atlanta, GA.

[4] P. M. Rinard. 1991. "Application Guide to Shufflers." Rep. No. LA-13819-MS. Los Alamos National Laboratory, Los Alamos, NM.

[5] A. L. Nichols, D. L. Aldama, and M. Verpelli. 2008. "Handbook of Nuclear Data for Safeguards: Database Extensions." Rep. No. IAEA INDC(NDS)-0534 IAEA Nuclear Data Section, Vienna, Austria.

[6] Python Software Foundation. 2017. "Python Language Reference." Version 3.5. Available at http://www.python.org, 2017.

[7] J. T. Caldwell, W. E. Kunz, and J. D. Atencio. 1984. "Apparatus and Method for Wuantiative Assay of Generic Transuranic Wastes from Nuclear Reactors." US Patent 4,483,816, issued November 20.

[8] K.-N. Leung. 2016. "Compact Neutron Generators,"Berkeley Lab, [Online]. Available: http://ipo.lbl.gov/lbnl1764/.

[9] R. D. McElroy Jr., and S. Croft. 2014. "Preliminary Performance Results for a Direct Multiplication Measurement for Use in Neutron Multiplicity Analysis." In *Proceedings of the International Nuclear Materials Management 55th Annual Meeting*, Atlanta, GA, July 20–24.

[10] D. Davidson, R. D. McElroy Jr., D. Brochu, and M. Villani. 1995. "A New 208 Liter Drum Neutron Coincidence Counter with Add-a-Source Matrix Correction." In *Proceedings of the 36th Annual Meeting for the Institute of Nuclear Materials Management*, Desert Springs, CA, July 9–12.

[11] H. O. Menlove, J. Baca, W. Harker, K. E. Kronke, M. C. Miller, S. Takahashi, K. Kobayashi, S. Seki, K. Matsuyama and A. S. Kobayashi. 1992. "WDAS Operation Manual Including the Add-A-Source Function." Rep. No. LA-12292-M. Los Alamos National Laboratory, Los Alamos, NM.

[12] N. Ennslin, W. C. Harker, M. S. Krick, D. G. Langner, M. M. Pickrell, and J. E. Stewart. 1998. "Application Guide to Neutron Multiplicity Counting." Rep. No. LA-13422-M Los Alamos National Laboratory, Los Alamos, NM.

[13] S. Croft, A. Favalli, and R. D. McElroy Jr. 2015. Unpublished report, Oak Ridge National Laboratory, Oak Ridge, TN.

[14] M. S. Krick, D. G. Langner, and J. E. Stewart. 1997. "Energy-Dependent Bias in Plutonium Verification Measurements Using Thermal Neutron Multiplicity Counters." Rep. No. LA-UR-97-3427. Los Alamos National Laboratory, Los Alamos, NM.

[15] H. Menlove. 1979. "Description and Operation Manual for the Active Well Coincidence Counter." Rep. No. LA-7823-M. Los Alamos National Laboratory, Los Alamos, NM.

[16] P. Rinard. 2001. "Application Guide to Shufflers." Rep. No. LA-13819-MS. Los Alamos National Laboratory, Los Alamos, NM.

[17] J. S. Hendricks, G. W. McKinney, L. S. Waters, T. L. Roberts, H. W. Egdorf, J. P. Finch, H. R. Trellue, E. J. Pitcher, D. R. Mayo, M. T. Swinhoe, S. J. Tobin, and J. W. Durkee. 2002. MCNPX Version 2.5. Rep. No. LA-UR-02-7086 Los Alamos National Laboratory, Los Alamos, NM.

[18] M. Tolbert. 1999. "New Brunswick Laboratory Certified Reference Material Certificate of Analysis." New Brunswick Laboratory, Argonne, IL.

[19] Canberra Industries. 2015. "Model JCC-31 High Level Neutron Coincidence Counter Specification Sheet," Available: http://www.canberra.com/products/waste_safeguard_systems/pdf/JCC-31-SS-C36906.pdf.

[20] E. F. Shores. 2002. "SOURCES 4C: A Code for Calculating (α,n), Spontaneous Fission." Rep. No. LA-UR-02-1839. Los Alamos National Laboratory, Los Alamos, NM.

[21] R. D. McElroy Jr., and S. Croft. 2012. "The Role of Active Neutron Interrogation to Safeguards Non-Destructive Assay (NDA) in the Post He World," in The *53rd Annual Meeting of the Institute of Nuclear Materials Management*, Orlando, FL.

[22] T. W. Crane. 1981. "Test andEvaluation Results of the ^{252}Cf Shuffler at the Savannah River Plant." Rep. No. LA-8755-MS. Los Alamos Scientific Laboratory, Los Alamos, NM.

[23] M. A. Schear, and S. J. Tobin. 2009. "Replacing a ^{252}Cf Source with a Neutron Generator in a Shuffler: A Conceptual Design Performed with MCNPX." Rep. No. LA-UR-09-03499." Los Alamos National Laboratory, Los Alamos, NM.